A review study on the use of dimethyl ether in diesel engines: effects on CO₂ emissions

İsmet Sezer

Department of Mechanical Engineering, Gümüşhane University, Gümüşhane, Turkey, isezer@gumushane.edu.tr, ORCID: 0000-0001-7342-9172

A B S T R A C T

Emissions from vehicles and other fuel combustion systems can alter the composition of the atmosphere and augment its capacity to absorb heat. These gases, which are effective at trapping heat, are known as greenhouse gases and include all gases found in vehicle emissions. Reducing the emissions of carbon dioxide (CO_2) has become an urgent necessity around the world, and many countries have imposed limits on their CO2 output. Using biofuels in automotive engines is an effective way of reducing greenhouse gas emissions. The CO_2 emissions emitted from the combustion of biofuels are absorbed as trees and plants grow. Biofuels can be used either as pure fuels or blended with conventional fuels. Most research has declared that the most effective way to reduce greenhouse emissions is the use of various biofuels. Therefore, it is essential to assess the outcomes of research regarding alternate fuels or fuel additives to determine their proper utilization. Using of diesel engines can also help reduce CO_2 emissions as they emit less CO_2 emissions than gasoline engines. This review study investigates the effects the using of dimethyl ether on CO_2 emissions in diesel engines. The results showed that CO_2 emissions decrease when using the pure DME and DME blends with diesel and LPG fuels due to the oxygen content and the lower carbon to hydrogen ratio of DME. The decrements in CO_2 emissions for pure DME, diesel–DME blends and LPG–DME blend are about 5.2–18.3%, 3–41.6% and 10.6–16.4%, respectively.

1. Introduction

Diesel engines are the dominant power sources among automobile engines due to their superior performance, fuel economy and lower emission of hydrocarbons (HCs), carbon monoxide (CO) and carbon dioxide (CO2) compared to gasoline engines [1]. However, diesel engines are currently known to emit higher levels of particulate matter (PM) and nitrogen oxides (NOx) emissions than those of gasoline engines. Therefore, to reduce emissions from diesel engines, numerous researches have been conducted, and progressive studies on alternative fuels have been carried out [2]. Among the various alternatives, DME stands out from the standpoint of energy security, as it can be industrially synthesized from coal, natural gas, and numerous types of biomass [3]. However, the physical properties of DME such as lower viscosity, lubricity, combustion enthalpy, and boiling point require modifications to the diesel engine structures and components. The technology for using pure DME in compression ignition (CI) namely diesel engines and vehicles are still in the development stage. However, DME can be used as an additive in diesel fuel or other alternative fuels [4]. It is

essential to evaluate the results of different studies concerning the use of DME in diesel engines together in order to apply them in practice. Therefore, this review study aims to investigate the effects of dimethyl ether on CO2 emission in diesel engines.

2. Characteristics of dimethyl ether

DME is the simple ether with the chemical formula of CH3–O–CH3 (C2H6O) as seen in the Fig. 1. In general, the physical properties of DME are very similar to those of the liquefied petroleum gas (LPG). Therefore, the requirements of the storage, fuel handling and transportation for DME are similar to those of LPG [3].
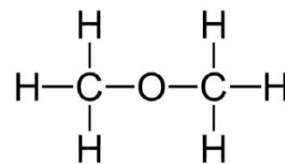

Figure 1. *Chemical structure of DME [5]*

DME can be produced using indirect or direct synthetic methods as seen in Fig. 2. DME is generated through a dehydration reaction after the synthetic reaction of methanol in the indirect synthetic method, while it is directly produced from natural gas in the direct synthetic method [5]. The production cost of DME is less than diesel fuel or gasoline on an energy equivalent basis. The economics of DME production are similar to compressed natural gas (CNG) or liquefied natural gas (LNG), when the large scale plants are considered [6]. DME is gaseous and almost non–toxic at atmospheric pressure and room temperature. Therefore, it needs to be pressurized over 0.5 MPa to keep it in a liquid state under ambient temperature and pressure conditions. The fuel delivery pressure should be increased to 1.7–2.0 MPa under engine operating conditions to prevent vapor lock in the fuel injection system [7, 8].
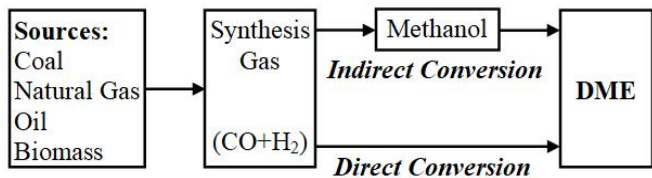

Figure 2. *Production methods of DME [9]*

The properties of DME and diesel fuel are tabulated in Table 1. It can be seen that the properties of DME are quite different from those of diesel fuel. DME has the high vapor pressure and low boiling temperature, which is a gas fuel at room temperature and atmospheric pressure. The heating value of DME is significantly lower than conventional diesel fuel. Therefore, the fuel supply system, injection system and combustion system of the engine should be redesigned or modified for the use of DME [10]. However, the cetane number of DME is higher than that of diesel fuel, which demonstrates good ignition capability. The latent heat of evaporation of DME is much higher than diesel fuel, which is beneficial for reducing the mixture temperature and increasing engine volumetric efficiency.

Table 1. *The properties of DME and diesel fuel [8]*

Property	DME	Diesel
Chemical formula	$CH_3–O–CH_3$	C_xH_y
Molecular weight, g/mol	46.07	170
Boiling point, °C	–24.9	180–360
Vapor pressure, kPa	530	<<10
Liquid density, kg/m³	668	840
Liquid viscosity, cP	0.15	4.4–5.4
Lower heating value, kJ/kg	28430	42500
Ignition temperature, °C	235	250
Cetane number	55–60	40–55
Stoichiometric air/fuel ratio	9	14.6

Modulus of elasticity, N/m²	6.37×10^8	1.486×10^9
Mass fraction of carbon	52.2	86
Mass fraction of hydrogen	13	14
Mass fraction of oxygen	34.8	0

DME has only C–H and C–O bonds, without C–C bonds, and contains about 34.8% oxygen. Because of these properties, DME combustion produces almost zero PM emission and the low noise level. It can tolerate a higher EGR rate to reduce NOx emissions greater extent than with conventional diesel fuel [6]. The other advantage of DME is that it is non–corrosive to the fuel system structure and metal surfaces [5]. The low viscosity of DME causes leakage in the fuel supply system, which relies on small clearances for sealing. Its lower lubricity characteristics result in intensified surface wear on the moving parts within the fuel injection system. Therefore, adding of proper additives is essential to prevent leakage and surface wear during the using of DME. The compressibility of DME is generally higher than that of diesel, so DME requires more compression pump work compared to the diesel. In general, DME deteriorates the rubber seals mainly due to its corrosive nature. For that reason, all existing rubber seals in injection systems should be replaced with non–corrosive materials [1].

3. Problems with dimethyl ether

DME has the favorable properties described above; there are some problems encountered in the practical use of DME such as below [4, 5].

• DME fuel feed pump and high pressure pump should be designed according to the requirements of the desired DME fuel system, engine power, and vehicle type. The design needs to account for the distinctive physical properties of DME, including its high vapor pressure, high compressibility, low viscosity, and its capacity to dissolve rubber and certain plastics.

• Due to its low viscosity, DME has poor lubricity which can cause frictional wear and internal leakage problems. To counter these issues, proper additives should be added to DME fuel. Furthermore, its high vapor pressure combined with its low viscosity can cause vapor locks and cavitations in fuel systems.

• DME has a lower heating value and density than diesel fuel, so more fuel needs to be injected to generate the same amount of heat. This means an increased injection rate and duration are necessary for DME compared to diesel fuel. This could, however, result in increased fuel line back pressure. Additionally, the use of larger fuel injectors, fuel pumps, and fuel tanks is essential when using of DME.

• The current ultra–high injection technology used for diesel fuel does not apply to DME injection due to the

superior atomization and vaporization characteristics of DME. Additionally, the o appropriate injector nozzle and combustion chamber geometry for DME should be determined for an optimum injection strategy.
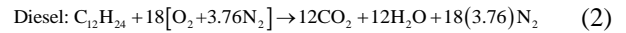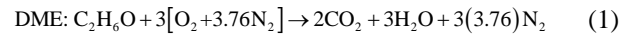
• The fuel heating may occur when engine temperature becomes high, which could result in a decrease in fuel density and an increase in compressibility. As a result, it becomes more difficult to supply the required amount of fuel to stabilize the DME engine operation. To mitigate this, the fuel cooling or temperature control unit is essential to the fuel supply and injection system in DME fuelled engines.

The ability to operate without causing black smoke makes DME a viable option in direct injection diesel engines. The only significant changes that need to be made are installing a high pressure (injection pressure no higher than 300 bar) fuel injection system, typically with an electronic control, in order to optimize the injection timing and duration. A turbocharger and an EGR system must be also added to take advantage of all the benefits of using DME. Finally, a suitable fuel storage and supply system must be put in place. These modifications can be done at a low cost without replacement of major engine components. Although optimization of the fuel injection equipment for overcoming issues such as low density, low lubricity, and corrosiveness is necessary for mass production, DME can be used with diesel or the other alternative fuels as an environmental friendly and renewable alternative fuel [4].

4. Researhes on dimethyl ether

There have been numerous studies conducted on the production technologies, fuel properties, combustion characteristics, engine performance, and exhaust emissions of DME. The different production methods were examined and compared in terms of cost in the studies of production technologies [9, 11, 12]. Moreover, the studies of fuel properties focused on features of DME which are different to diesel fuel, such as oxygen content, low density, low viscosity, and low lubricity [5, 13–15]. Additionally, the effects of DME on parameters such as injection characteristics [16–23], ignition delay, combustion duration, cylinder temperature, and pressure were investigated in the combustion studies [13, 24–36]. The studies of engine performance analyzed the impacts of DME on parameters such as torque, engine power,

brake thermal efficiency, and fuel consumption [37–58]. Further, the emission studies investigated the effects of DME on emissions of CO, HC, PM or soot, NOx, and CO2 [59–80]. The lower CO2 emissions are anticipated during the use of DME and its blends, since the combustion equations of DME and diesel fuels at stoichiometric conditions are as Eqs. (1) and (2) [13].

$$\text{DME: } C_2H_6O + 3\left[O_2 + 3.76N_2\right] \rightarrow 2CO_2 + 3H_2O + 3(3.76)N_2 \quad (1)$$

$$\text{Diesel: } C_{12}H_{24} + 18\left[O_2 + 3.76N_2\right] \rightarrow 12CO_2 + 12H_2O + 18(3.76)N_2 \quad (2)$$

Therefore, the potential of dimethyl ether on reducing of CO2 emissions in diesel engines was investigated in this review study based on literature.

5. Combustion characteristics of dimethyl ether

The 664 K can provide thermal reactivity energy for the breaking up of DME into CH4, H2 and CO. Comparing the combustion and decomposition of DME; it can be observed that the decomposition process occurs at different temperatures and pressures with varying speeds, while combustion takes place at cylinder temperature of approximately 1000 K. According to Eq. (3), which shows the decomposition of DME, each mole of DME is broken down into one mole of CH4, H2, and CO. The decomposition speed of DME is related to temperature; such as, chemical kinetic modeling of DME demonstrates that 99% of it is broken down in around 0.1 s when it is heated to 973 K, with the process being faster at higher pressures [81].

$$CH_3OCH_3 \rightarrow CH_4 + H_2 + CO \quad (3)$$
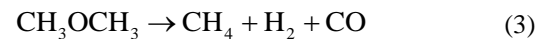
It is declared that the ignition of DME in combustion chambers occurs earlier than that of diesel or biodiesel fuels in CI engines, owing to its lower ignition temperature and higher cetane number. Effects of DME on the parameters related to the combustion of DME such as heat release, combustion pressure and temperature are presented below. Additionally, DME combustion is soot–free because of its lack of C–C bonds, and it has lower HC and CO emissions than those of diesel combustion. NOx emission from DME combustion can be reduced by applying exhaust gas recirculation ratio (EGR), as well as with the multiple injection strategy and premixed combustion [13].
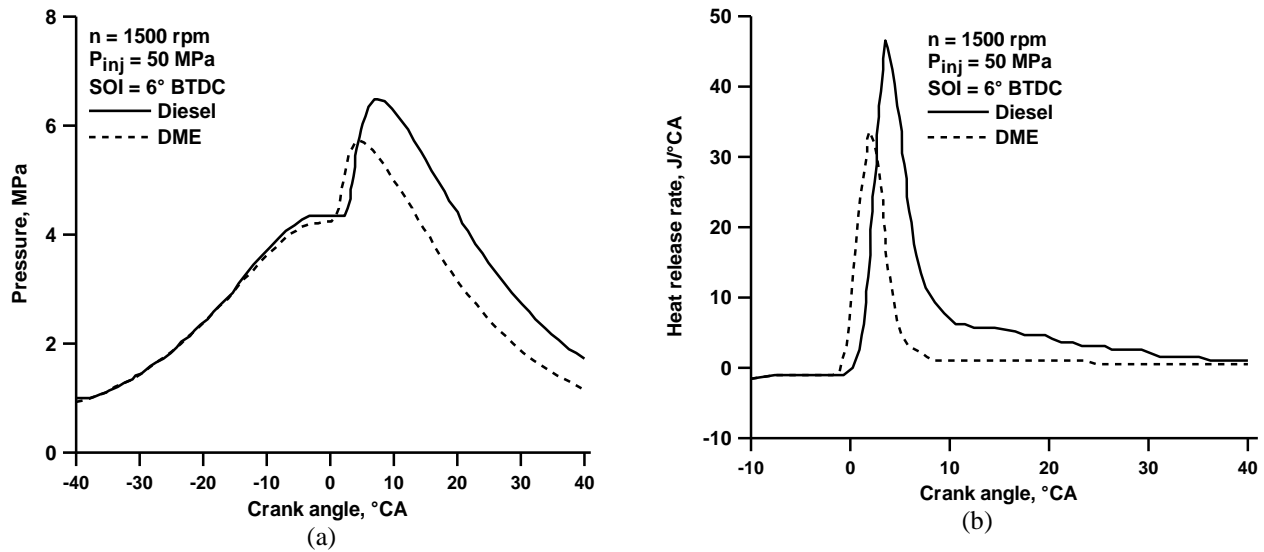
(a)   (b)

Figure 3. *Variation of a) pressure and b) heat release rate for Diesel and DME fuels [5]*

Fig. 3(a) and (b) show the combustion pressure and heat release rate (HRR) of DME and diesel fuels at engine speed of 1500 rpm, injection pressure of 50 MPa, start of injection (SOI) of 6° BTDC (before top dead center), and an injection fuel mass of 8 mg/cycle. The peak pressure of diesel fuel was higher than that of DME at the same injection quantity due to its higher lower heating value (LHV) of 42.5 MJ/kg compared to that of DME's 28.43 MJ/kg. However, it is declared that an increased amount of injected DME should match that of diesel to improve the combustion characteristics such as combustion pressure and heat release [5].

Fig. 4 (a) and (b) show the combustion characteristics of DME and diesel fuels for a single–cylinder engine with constant energy input at 50 MPa of injection pressure. In the case of DME fuel, the combustion pressure and heat release rate of the engine resulted in a higher peak compared to that of diesel fuel at injection timing of 2° BTDC as seen in Fig. 4 (a) and (b). Comparing the ignition characteristics of both DME and diesel fuel, DME combustion showed earlier ignition than diesel combustion because the cetane number of DME is higher than that of diesel fuel. The gap in the ignition delay between diesel and DME was about 1.3–2.3° CA (crank angle). Therefore, the shorter ignition delay and the faster ignition of DME created an excessive rise in pressure and heat release rate compared to diesel fuel, as seen in the combustion pressure profile and heat release pattern [13].
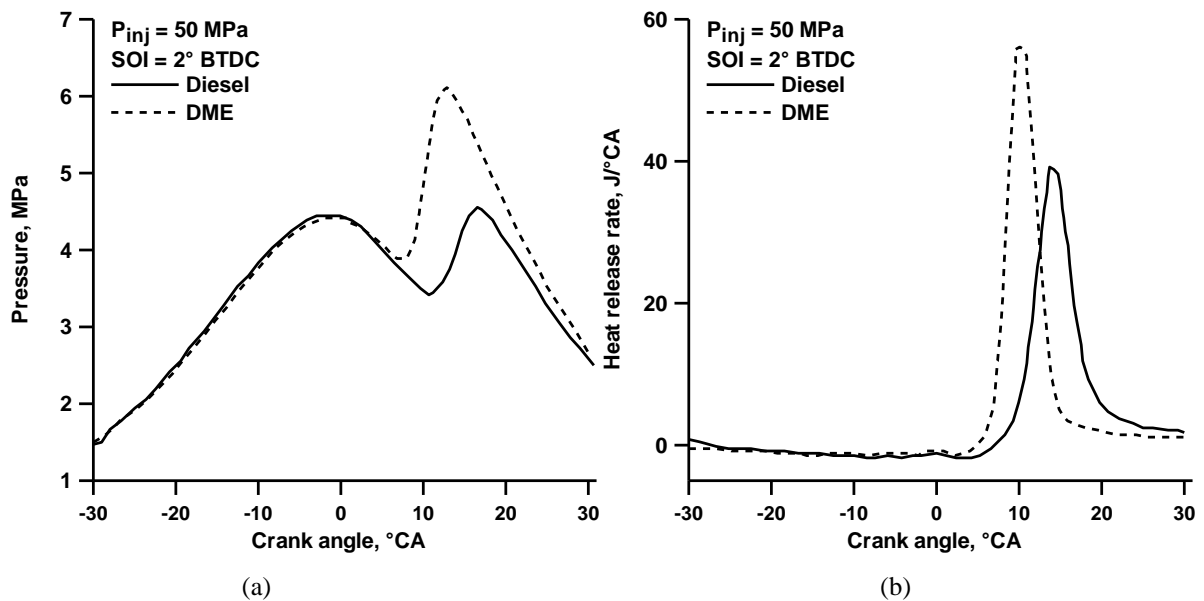

(a)   (b)

Figure 4. *Variation of a) pressure and b) heat release rate for Diesel and DME fuels [13]*

Fig. 5 shows a comparison of the combustion characteristics at baseline condition. It can be seen that the combustion pressure and heat release rates of diesel fuel have lower peaks than those of the DME fuel with the same calorific value due to the different combustion properties. In addition, the ignition timing of the DME fuel is more advanced than that of diesel fuel, as it has a higher cetane number and faster evaporation. Accumulated heat release (AHR) of DME fuel is also higher than that of diesel fuel due to the greater injected fuel amount. Finally, the accumulated heat releases of DME and diesel fuel become stable from 5° and 30° ATDC (after top dead center), respectively. This is due to the more rapid combustion of DME fuel resulting from its faster evaporation compared to diesel fuel [77].

Fig. 6 shows the comparison of combustion pressure and heat release rate for diesel, GTL (Gas to Liquid) and DME at the maximum torque point and 9° CA injection timing. It can be seen in 6(a) that the peak pressures of diesel, GTL, and DME were 13.9, 13.4, and 11.2 MPa respectively, with the maximum combustion pressures of GTL and DME being lower than that for diesel by 3.6% and 17.2% respectively. This is attributed to the significantly high cetane number of GTL and DME, leading to a shortened ignition delay period during which less combustible mixture is formed and the maximum combustion pressure drops. In addition, Fig. 6(b) reveals that the peak value of heat release rate with GTL is lower than that for diesel by 3.0%. The location of GTL heat release rate peak value is slightly delayed compared to diesel. The peak heat release rate of DME is also lower than that for the diesel engine and its peak heat release rate is later than that for diesel. This is due to the longer pressure wave propagation for GTL and DME in comparison to diesel, which results in a longer fuel injection delay for GTL and DME than for diesel. Consequently, the effect of the injection delay of GTL and DME is more pronounced and causes the lagged maximum pressure, even though GTL and DME, with high cetane numbers, should have a prompt combustion [67].
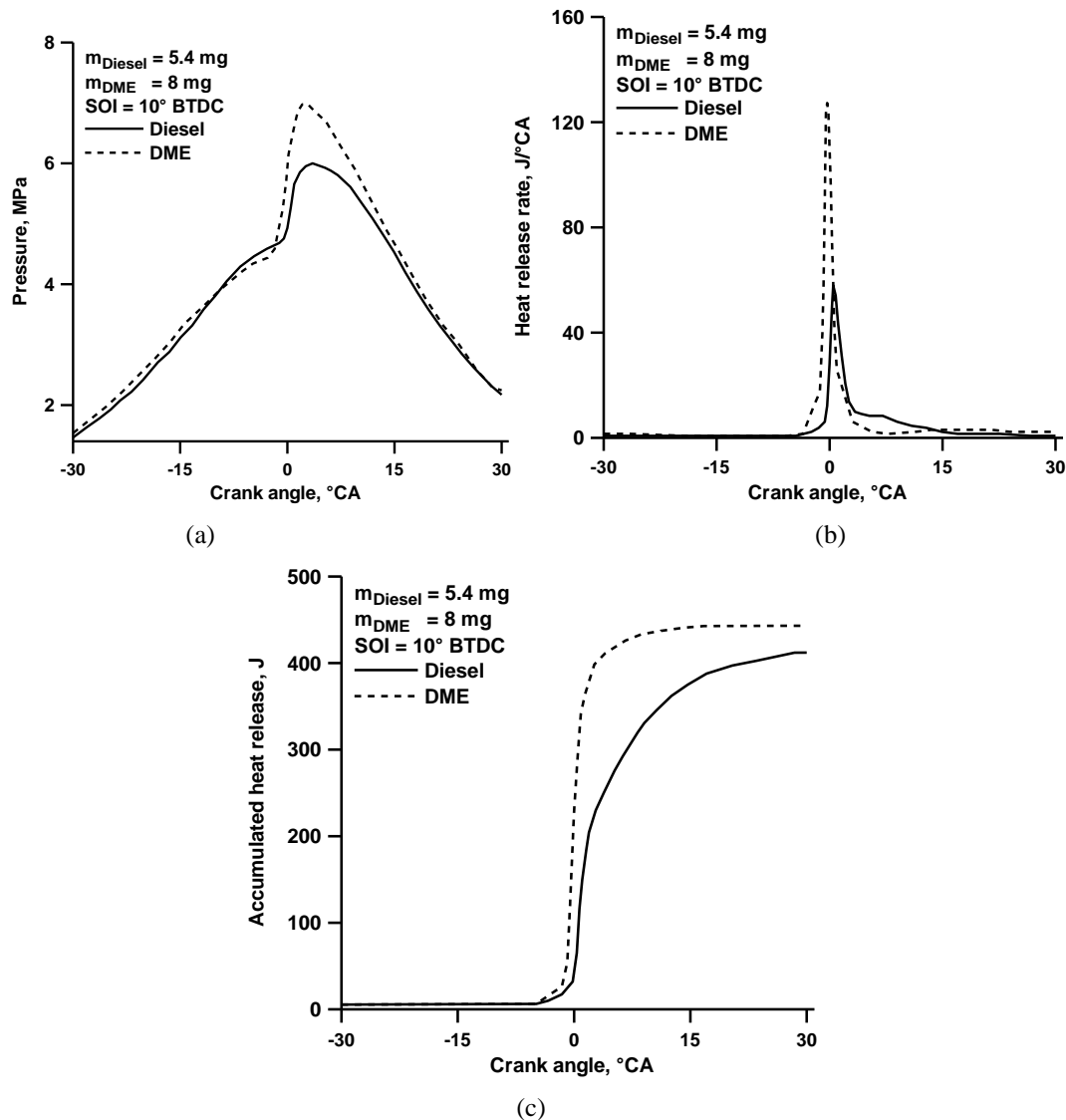

(a)

(b)

(c)

Figure 5. *Variation of a) pressure, b) heat release rate and c) accumulated heat release for Diesel and DME fuels [77]*

(a)   (b)
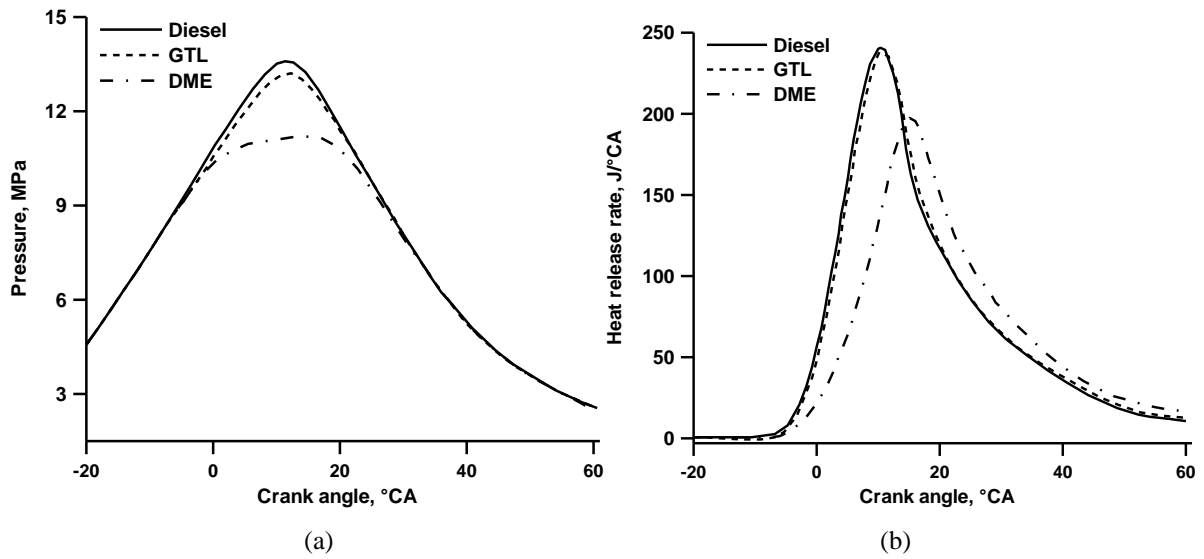
Figure 6. *Variation of a) pressure and b) heat release rate for Diesel, DME and GTL fuels [67]*

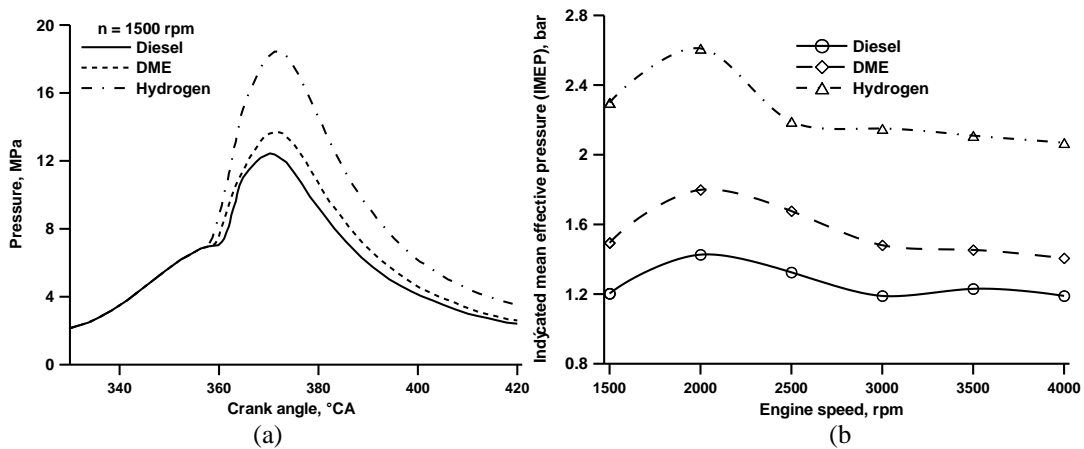(a)   (b)

Figure 7. *Variation of a) pressure and b) IMEP for Diesel, DME and Hydrogen fuels [49]*

Fig. 7(a) compares the pressure for different fuels at 1500 rpm crank angle. Fig. 7(a) shows that hydrogen fuel combustion produces higher pressure and temperature within the cylinder in comparison to the other fuels. This higher temperature and pressure contributes to higher engine efficiency. Furthermore, Fig. 7(b) indicates that hydrogen fuel can create a higher IMEP (indicated mean effective pressure) compared to the other fuels. However, a decreasing trend of IMEP can be observed after 2000 rpm as the engine speed increases. At 4000 rpm, 46.8% and 18% IMEP increase of hydrogen to DME and DME to diesel application were obtained, respectively. The higher IMEP of hydrogen can be attributed to its higher latent enthalpy and chemical composition. Consequently, higher mean effective pressure results in shorter energizing time and prolonged premixed combustion duration [49].
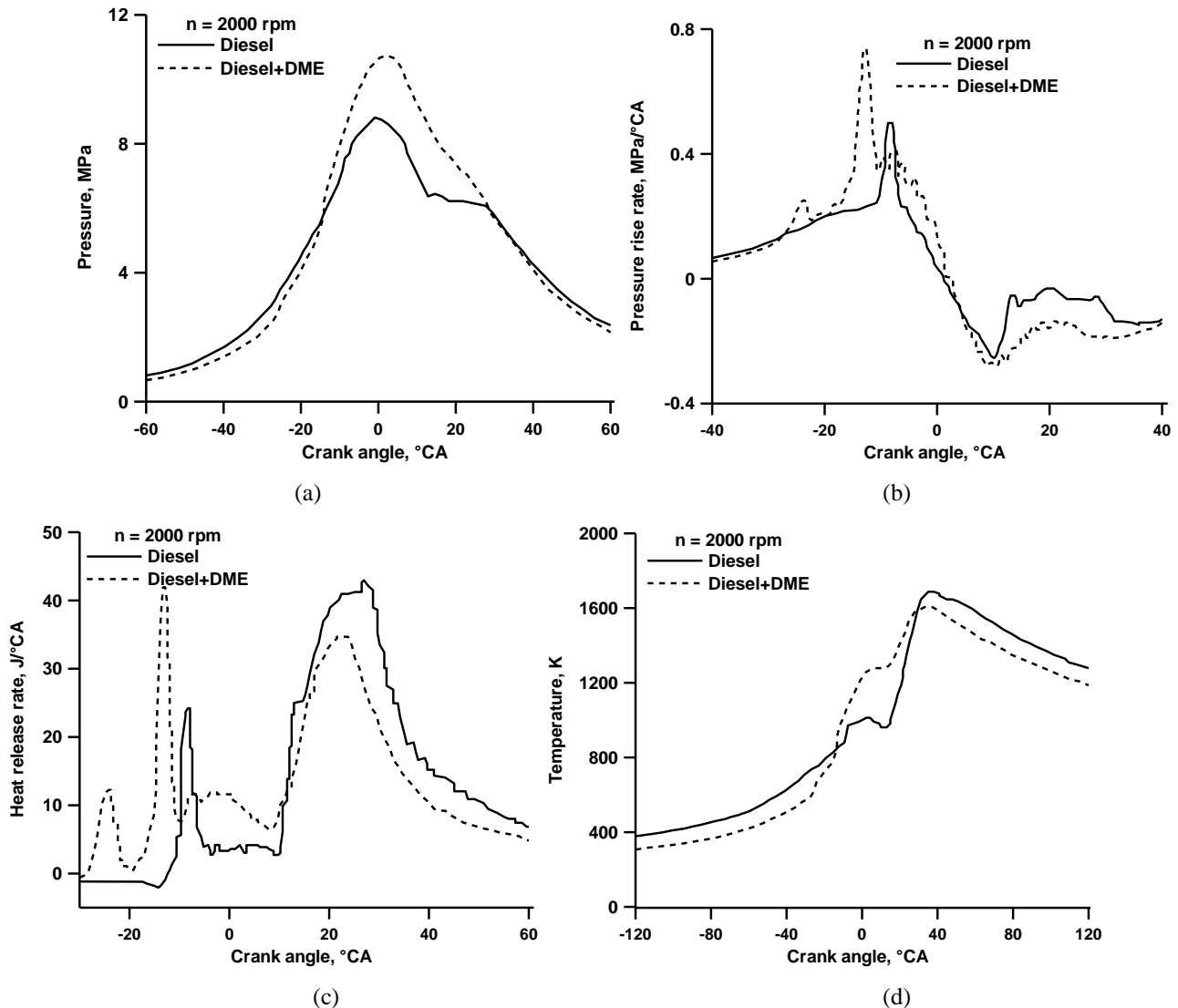
Figure 8. *Variation of a) pressure, b) pressure rise rate, c) heat release rate and d) temperature for*

Diesel and Diesel–DME blend [7]

Fig. 8(a) shows that in premixed charge compression ignition (PCCI) composite combustion mode of Diesel–DME blend and direct injection (DI) combustion of diesel fuel, the maximum pressure is 10.7 MPa and the corresponding crank angle of 1.9° ATDC for Diesel–DME, which is higher than the peak pressure of 9.0 MPa for DI combustion at 0.6° ATDC. However, the maximum pressure appears slightly delayed due to DME forming a homogeneous mixture before entering the cylinder and its low ignition temperature causing early combustion at the end of the compression stroke. Fig. 8(b) illustrates the difference between Diesel–DME and diesel fuel pressure rise rate, where the peak pressure rise rate of Diesel–DME is 0.732 MPa/°CA and that of diesel fuel is 0.527 MPa/°CA, with the peak rate moving from 8.2° BTDC to 12.7° BTDC. It is therefore important to pay attention to the supply amount of DME when running the engine in the composite combustion mode. Otherwise, power performance

and fuel economy will be adversely affected. Fig. 8(c) shows the variation of heat release rate between two combustion modes. It is seen that a great difference exists between the heat release rate of the composite combustion mode and the diesel DI combustion mode. The heat release in the composite combustion mode comprises three stages. The first stage involves low temperature combustion at compression pressures between 30° and 20° BTDC. The second stage, with the cylinder temperature increasing, involves the mixing and ignition of DME and pilot diesel injection, with the corresponding compression pressure being between 20° and 10° BTDC. This is mainly a short duration combustion process with a higher heat release peak. The third stage involves combustion after diesel injection. The heat released by the diesel DI combustion consists of two parts: the first part is released by the pilot injection of the first stage, the second part by the main injection. Fig. 8(d) illustrates that the cylinder

temperature in the composite combustion mode is lower than in the diesel DI mode before 15° BTDC. The cylinder temperature in the composite combustion mode is higher than that in the diesel DI mode between 15° BTDC and 30° ATDC. The cylinder temperature of the composite combustion mode is lower than that of the diesel DI mode after than around 30° ATDC. The maximum average cylinder temperature in both combustion modes occurs when the CA of 30° ATDC. The maximum temperature of the diesel DI mode is 1650 K, which is higher than 1600K of composite combustion mode [7].
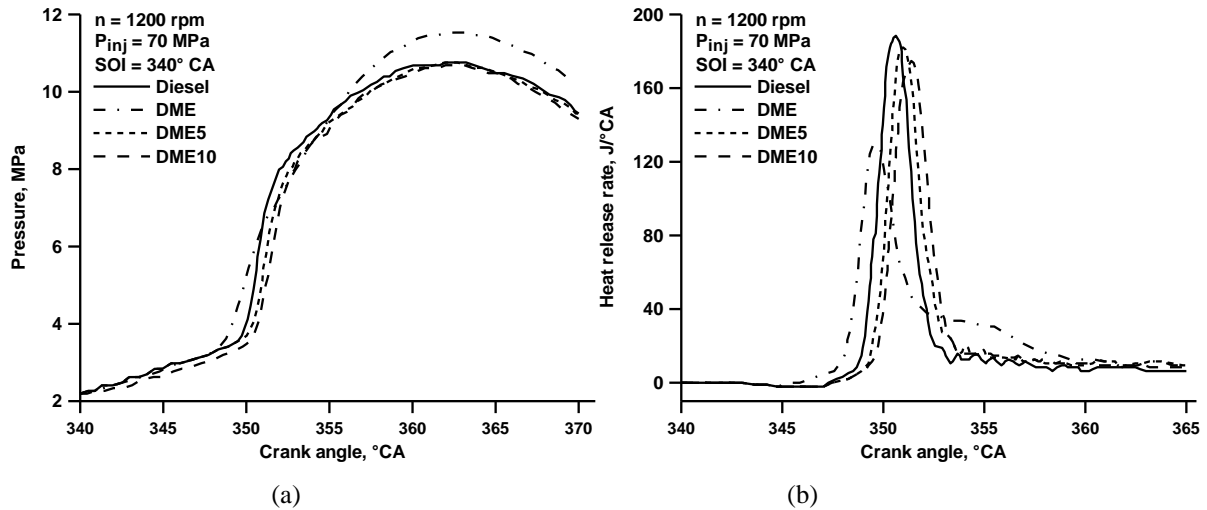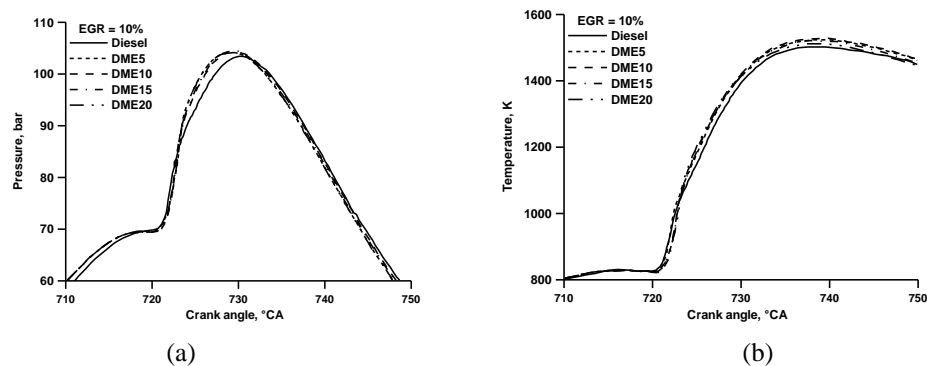

Figure 9. *Variation of a) pressure and b) heat release rate for Diesel–DME blends [20]*

Fig. 9(a) and (b) show the cylinder pressure and heat release rate traces for diesel fuel, DME and diesel–DME blends at injection timing of 340° CA. It is seen that the peak pressure with DME was higher by 1 MPa than those of the diesel fuel and DME blends. This is attributed to the rapid vaporization, high cetane number and good mixing of DME. The peak cylinder pressures for the DME blends were similar to that for diesel fuel. In terms of the slope of the pressure curve, the diesel fuel had the steepest one, whereas the slope of the pressure curve for DME blends became smoother as the DME ratio increased. The ignition delay of DME is shorter than that of the diesel fuel due to fast vaporization as seen in heat release rate graph. However, ignition delay was longer than that of the diesel fuel when the DME blends were injected into the cylinder. This can be explained that the diesel fuel and air in the cylinder were inhibited by the earlier vaporization of the DME fuel. Additionally, the ascending order of the slope of the heat release rate was diesel fuel, DME5, DME10 and DME, with the heat release rate curve gradient for the diesel fuel being the steepest [20].
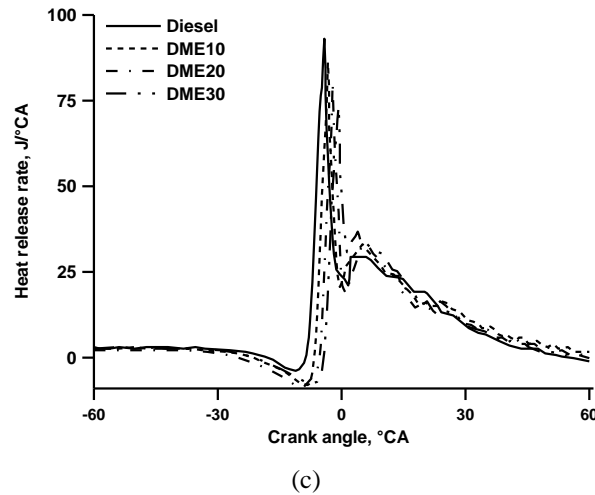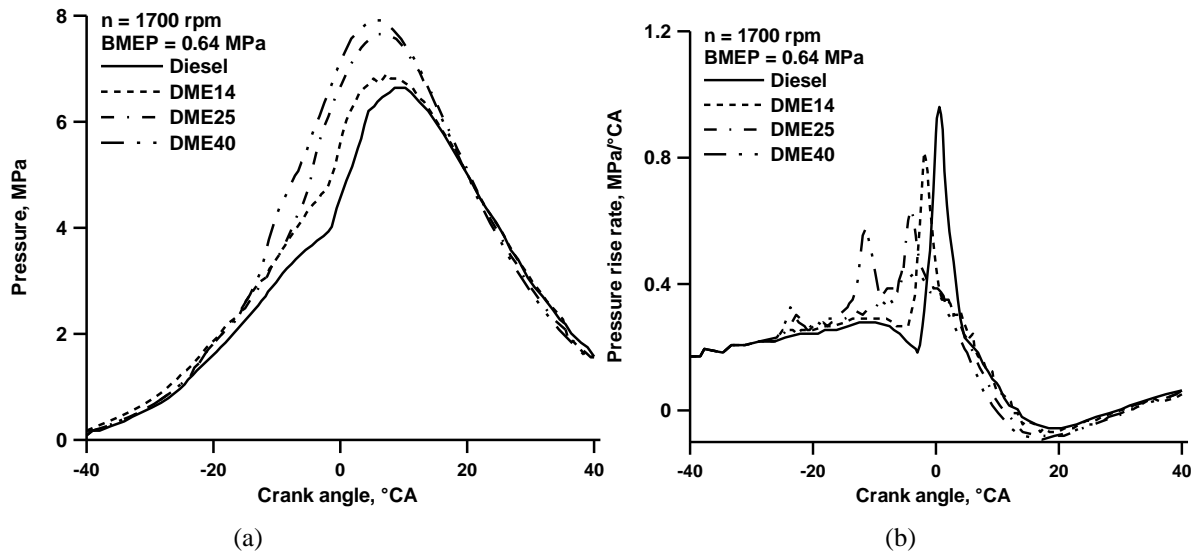
(c)

Figure 10. *Variation of a) pressure and b) temperature for Diesel and Diesel–DME blends [33] and c) heat release rate for Diesel and Diesel–DME blends [66]*

Fig. 10(a) depicts the impact of various diesel–DME blends on cylinder pressure, with peak pressure increasing as the ratio of DME in diesel blend increases due to a decrease in ignition delay. Fig 10(b) illustrates the effect of various diesel–DME blends on cylinder temperature, which is higher for higher DME blend ratio as DME is being combusted more efficiently [33]. Fig. 10(c) illustrates the heat release rate of four different fuels. It is observed that the amount of heat released during the premixed combustion stage when using diesel–DME blends is lower than that of diesel fuel. This decrease in heat release leads to a reduction in combustion pressure and temperature, consequently resulting in lower NOx emission. With an increase in DME content, there is a decrease in the amount of heat release during the premixed combustion stage due to the improved auto–ignition and atomization properties of DME in the diesel–DME blends, consequently improving engine combustion [66].
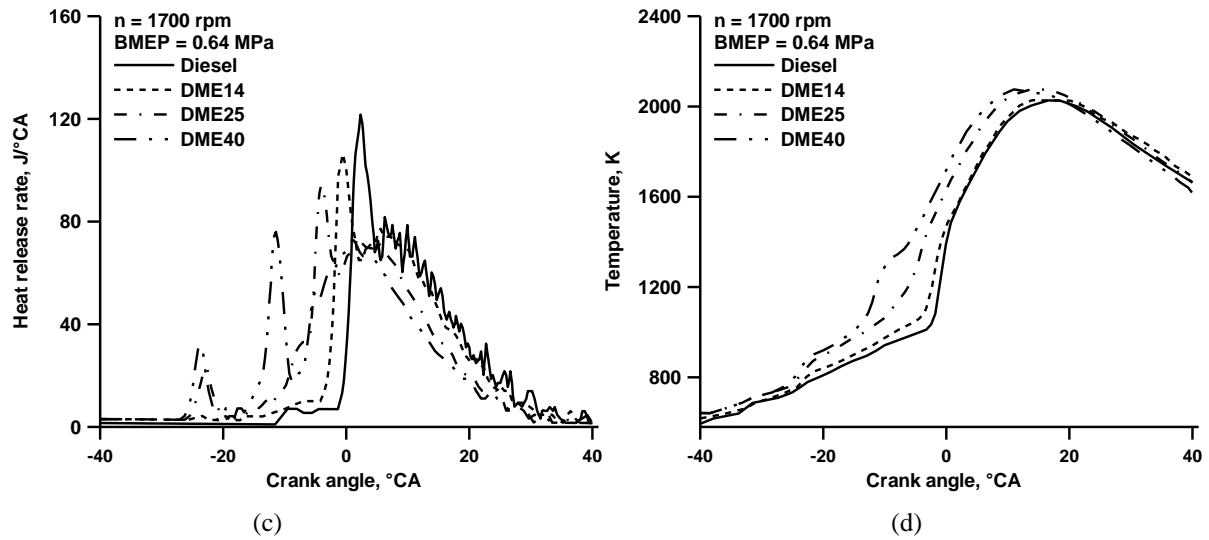

(a)

(b)

(c)

(d)

Figure 11. *Variation of a) pressure, b) pressure rise rate, c) heat release rate and d) temperature for Diesel and Diesel–DME blend [45]*

Fig. 11(a) shows based on analysis of measured indicator diagrams, the remarkable distinctions in values and positions of maximum pressure (pmax) under various port DME energy ratios. It is clear that, due to the DME's ability to auto–ignite easily when mixed with intake air, the ignition timing of DME is prior to that of diesel and the initial combustion occurs in a homogenous charge compression ignition (HCCI) process. This is seen in the cylinder pressure curves, which display an increased pressure peak as well as an advanced position of that peak when DME is fumigated in the intake air. For both port inspiration and in–cylinder injection DME, pmax increases with the amount of DME–premixed. Fig. 11(b) reveals the relationship between pressure rise rate and DME energy ratio. This curve displays the level of pressure oscillations as well as other combustion characteristics. For conventional direct injection compression ignition (DICI), only one peak is present in the rate of pressure rise curve. However, as DME–diesel dual fuel PCCI combustion occurs sequentially between HCCI and DICI, more peaks than one are visible in the rate of

pressure rise curve. The first peak, during cool flame process, stays relatively constant in crank angle, but increases with the DME energy ratio. The peak moves to an earlier crank angle and decreases in value as more DME is added during the diffusive combustion process. The heat release curves of DME–diesel dual fuel PCCI combustion cases were complex, unlike typical DICI combustion. As shown in Fig. 11(c), the heat release process consisted of three stages: cool flame, HCCI combustion, and diffusive combustion. It was observed that the timing of the cool flame was almost consistent regardless of the DME energy ratio. Moreover, the negative temperature coefficient region shortened and the HCCI combustion was advanced as more DME was added. Simultaneously, maximum heat release rate of DME cool flame and high temperature reaction increased but maximum heat release rate of diesel diffusion decreased with increase in DME energy ratio. In Fig. 11(d), the in–cylinder temperatures were shown to be higher due to the DME HCCI combustion, as the DME energy ratio increased [45].
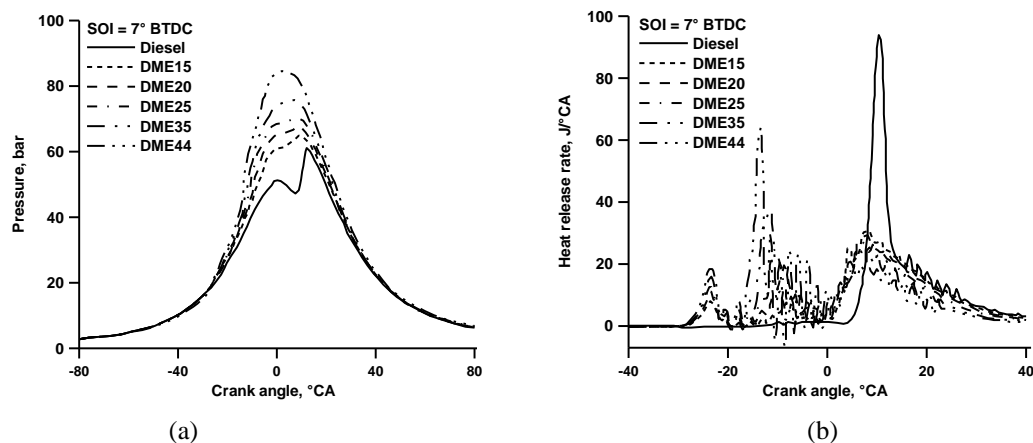

(a)

(b)

Figure 12. *Variation of a) pressure and b) heat release rate Diesel–DME blends [34]*

Fig. 12(a) shows the variation of cylinder pressure with the increasing of DME ratio. As DME is injected in the intake air, it undergoes a premixed combustion process, which leads to an earlier start of combustion, and an increased peak pressure, as evidenced by the pressure trace. This is further supported by the heat release rate in Fig. 12(b). Without DME addition, no heat release is observed until the mild premixed ignition at around 2° BTDC, while with DME addition, there is an early start of combustion at 32° BTDC, bringing with it low temperature heat release, which intensifies with increasing DME fumigation. A second stage of DME oxidation, starting between 22° BTDC and 5° BTDC and mostly in advance of the diesel fuel injection event at 7° BTDC, is also noted. At 15% DME ratio, the second stage of DME oxidation begins just as the diesel fuel injection starts at 7° BTDC, while at 20% DME ratio, it happens earlier at around 10° BTDC. This second stage oxidation further moves to earlier timing and increasing peak heat release rate with more DME added, which leads to a substantial increase in peak cylinder pressure of 33% at 44% DME ratio [34].
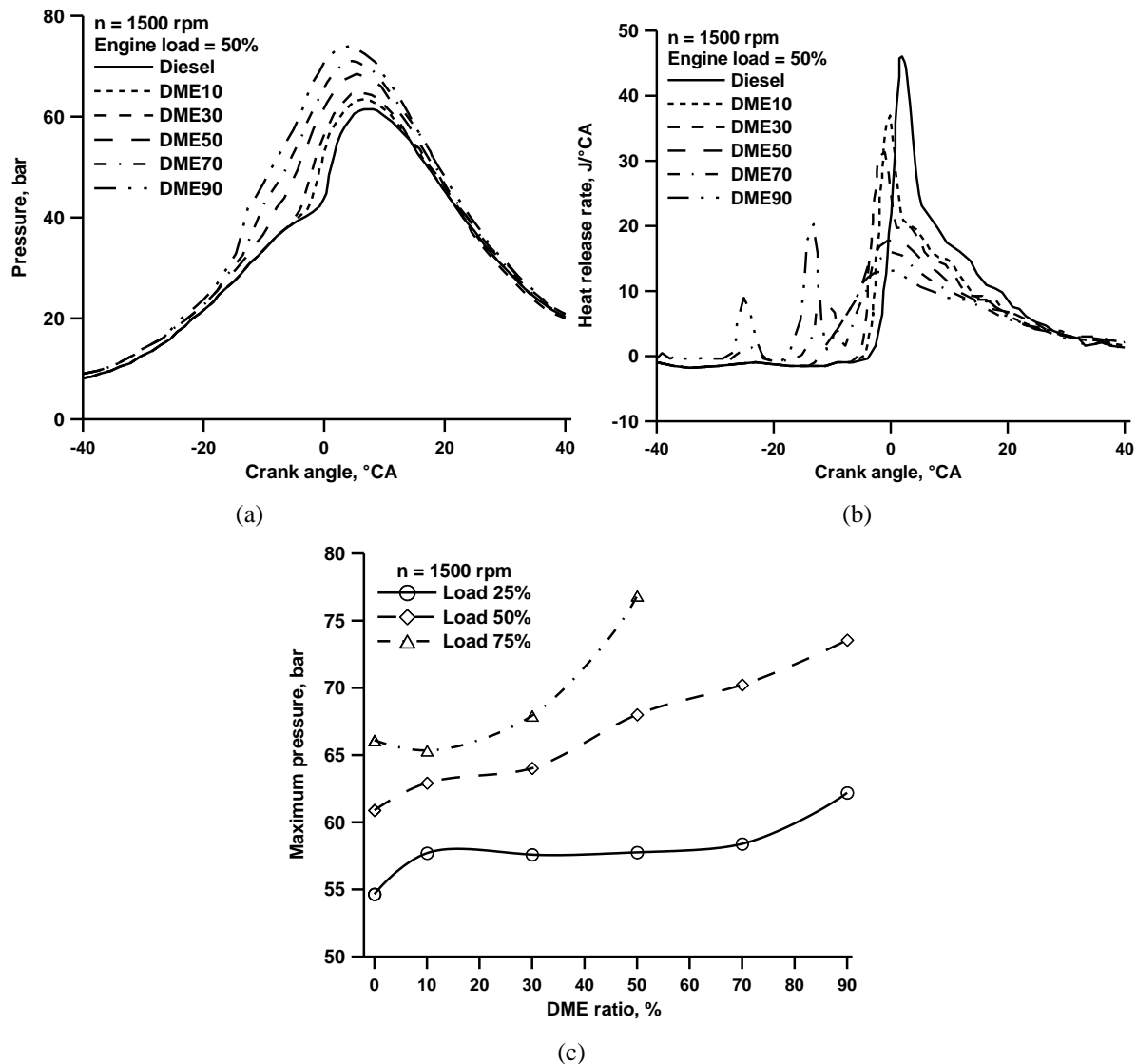

(a)

(b)

(c)

Figure 13. *Variation of a) pressure, b) heat release rate and c) maximum pressure for Diesel and Diesel–DME blends [52]*

The effect of PCCI with dual fuel (DME and diesel) on cylinder pressure and heat release rate characteristics are depicted in Fig. 13(a) and (b). The 100 consecutive engine cycles analysis, which included peak engine cylinder pressure and heat release rate, was conducted to analyze entire HCCI and diffusion combustion characteristics. In DME–diesel dual fuel mode of PCCI engine, two peak heat release rate curves were observed. The first peak pressure was due to the low–temperature combustion induced by DME injection. This HCCI combustion, which was characterized by high cetane number and auto–ignition temperature, was suitable for the application. The reaction occurred from 29° BTDC to 24°

BTDC, in which DME was combusted at the appropriate temperature. Higher DME concentration led to increased peak heat release rate in the low temperature combustion, without significant differences with the engine load. The second peak pressure was a result of diffusion combustion of diesel fuel. The second peak of heat release rate from diffusion combustion decreased with larger amount of DME pre–mixing ratio, due to the reduced diesel fuel concentration. The maximum peak pressure at 50% load was closely at top dead center (TDC), when the DME ratio was 90%. The ignition delay was reduced in comparison to neat diesel fuel, resulting in advanced peak pressure with any given engine speed and load. Fig. 13(c) illustrates that the maximum cylinder pressure varies depending on engine load and DME ratio. The high proportion of DME pre–mix increases the maximum peak pressure at all engine load conditions, as the pre–mix enhances combustion in the cylinder. At high load of 75% of maximum load however, it was found that the engine becomes unstable when using the high DME ratio (>50%) in port injection, due to the unmodified compression ratio; this can lead to engine knock. Thus, a low compression ratio is required for high DME ratio under high engine load conditions [52].
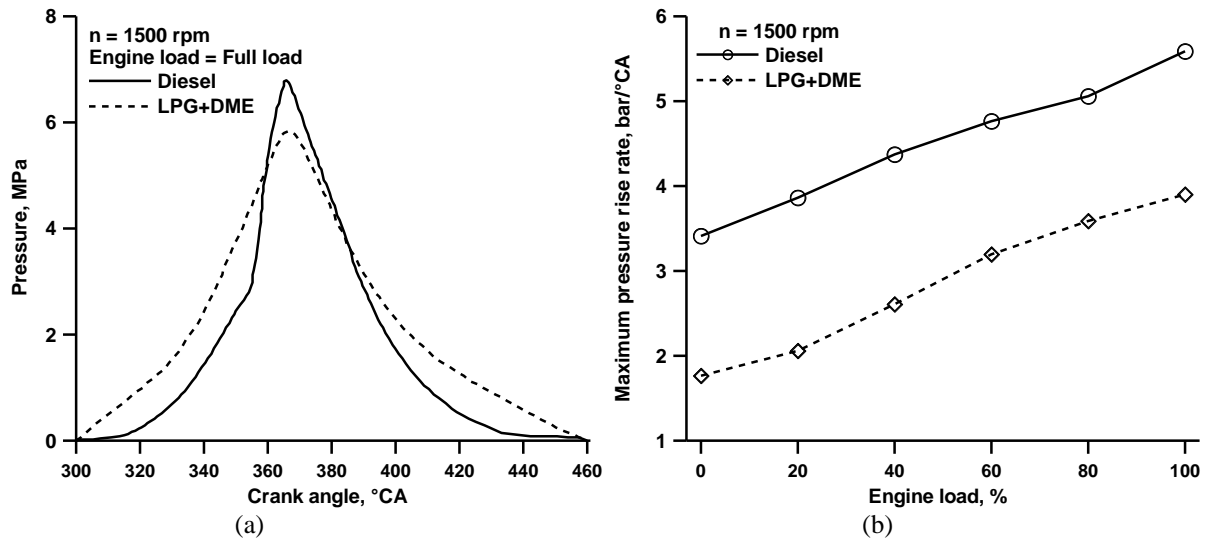

Figure 14. *Variation of a) pressure and b) rate of maximum pressure rise for Diesel and LPG–DME blend [24]*

The pressure crank–angle data for both diesel and LPG–DME operation at full load condition is depicted in Fig. 14(a). It is observed that diesel operation obtains a maximum cycle pressure of around 68 bar, while the maximum cycle pressure for LPG–DME operation is 44 bar. The reduced pressure in the LPG–DME fuel operation can be attributed to the decrease in heat release after TDC due to lower cylinder-gas temperature, which results in a decreased peak pressure. Fig. 14(b) shows the rate of maximum pressure rise for both diesel and LPG–DME operation. Diesel operation has a higher pressure rise rate compared to that of LPG with DME operation. This can be explained by the DME cooling of the intake charge and the consequently lower cylinder gas temperature, which leads to a lower pressure rise rate [24].
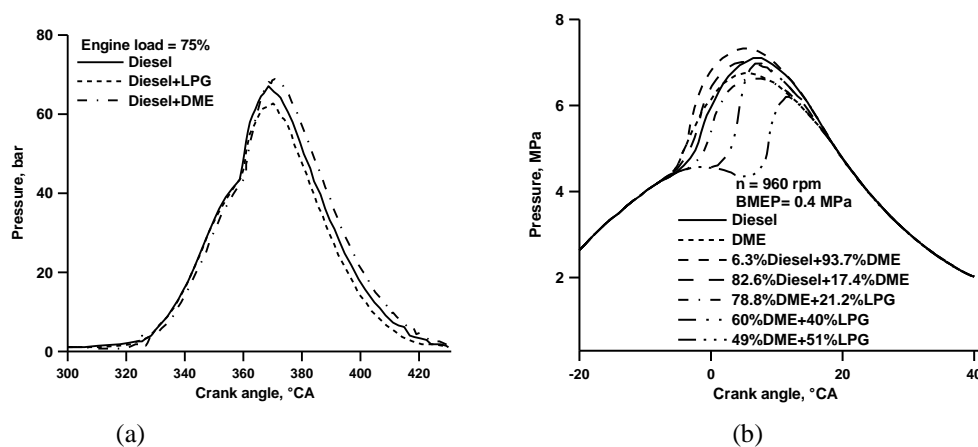

Figure 15. *Variation of pressure a) for Diesel, Diesel–LPG and LPG–DME blends [32] and b) for Diesel, Diesel–DME and DME–LPG blends [71]*

The cylinder pressure of diesel with DME and LPG without EGR, as reflected in Fig. 15(a), is positioned between diesel with DME and diesel with LPG due to the fuel physical and chemical properties such as density, viscosity, cetane number, boiling point and latent heat of vaporization, which can significantly affect combustion patterns. The lower boiling point and higher cetane number of DME can lead to improved combustion characteristics, such as advanced peak pressure of

up to 2° CA compared to diesel. Fig. 15(b) reveals the improved performance of DME blended diesel and LPG engines in terms of pressure against crank angle. The pressure characteristics of diesel engine is observed to remain unaffected, even slightly improved, while combustion properties are seen to be considerably improved with increased concentration of DME blended with LPG [71].
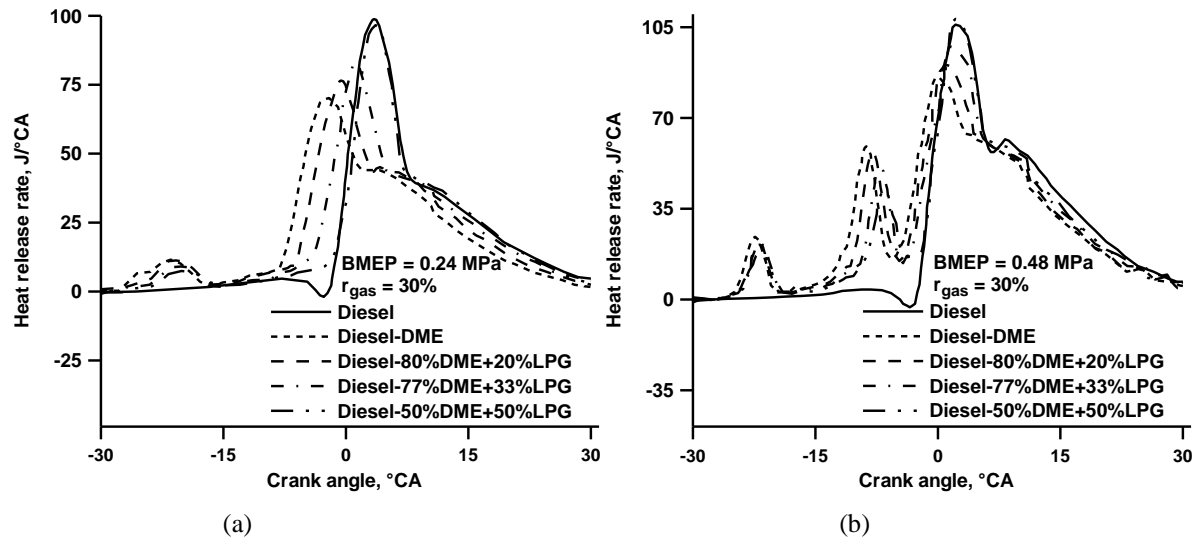

(a)   (b)

Figure 16. *Variation of heat release rate for Diesel–DME+LPG blends at a) BMEP of 0.24 MPa and b) BMEP of 0. 48 MPa [81]*

Fig. 16(a) gives the heat release process for a dual–fuel PCCI combustion engine with varying ratios of LPG at BMEP of 0.24 MPa and a gas fuels (DME and LPG) energy ratio of 30%. It can be seen that the heat release process consists of DME low temperature reaction (LTR) and conventional diffusion–controlled CI combustion. The ignition timing of the DME LTR combustion remains essentially constant (around 24–25° BTDC) regardless of the amount of premixed charge, as seen in Fig. 18(a). This is due to the fact that the initial combustion temperature of DME LTR combustion is usually around 700–750 K, and the ignition timing is mainly determined by the cylinder temperature, with the rise of temperature mainly influenced by the compression of the charge; this causes the ignition timing of the DME LTR combustion to be relatively unaffected by the quantity of premixed charge. The maximum value of the heat release rate during the DME LTR process decreases slightly with an increase in LPG ratio, as the quantity of DME available for auto–ignition reduces. Meanwhile, it can be observed that the start of CI combustion is postponed with a higher LPG ratio, as the premixed LPG prevents DME from auto–ignition and part of the energy or radicals released from the DME cool–flame are used to ignite the LPG when its quantity increases.

Additionally, the maximum value of the heat release rate increases slightly with the gas fuels ratio due to the higher lower heating value of LPG compared to DME. Fig. 16(b) shows the heat release process of the dual–fuel PCCI combustion engine with different LPG ratios at a BMEP of 0.48 MPa and a gas fuels energy ratio of 30%. It can be seen that with an increase in the amount of port fumigation DME, high temperature reaction (HTR) becomes more noticeable compared to that at a BMEP of 0.24 MPa and a gas fuels energy ratio of 30% and the heat release process of the dual–fuel combustion consists of LTR, HTR, and a conventional diffusion–controlled CI combustion. Similar to Fig. 18(a), the timing of LTR onset is nearly the same, and the maximum value of heat release rate during the DME LTR process slightly decreases with an increase in LPG ratio. Additionally, the onset of HTR is delayed, and the maximum value of heat release rate decreases slightly with a rise in LPG ratio due to the suppression of LPG addition on DME auto–ignition. The start of diffusion–controlled combustion is also delayed with a rise in LPG ratio, but the maximum value of heat release rate during this stage slightly increases due to the higher heating value of LPG [81].
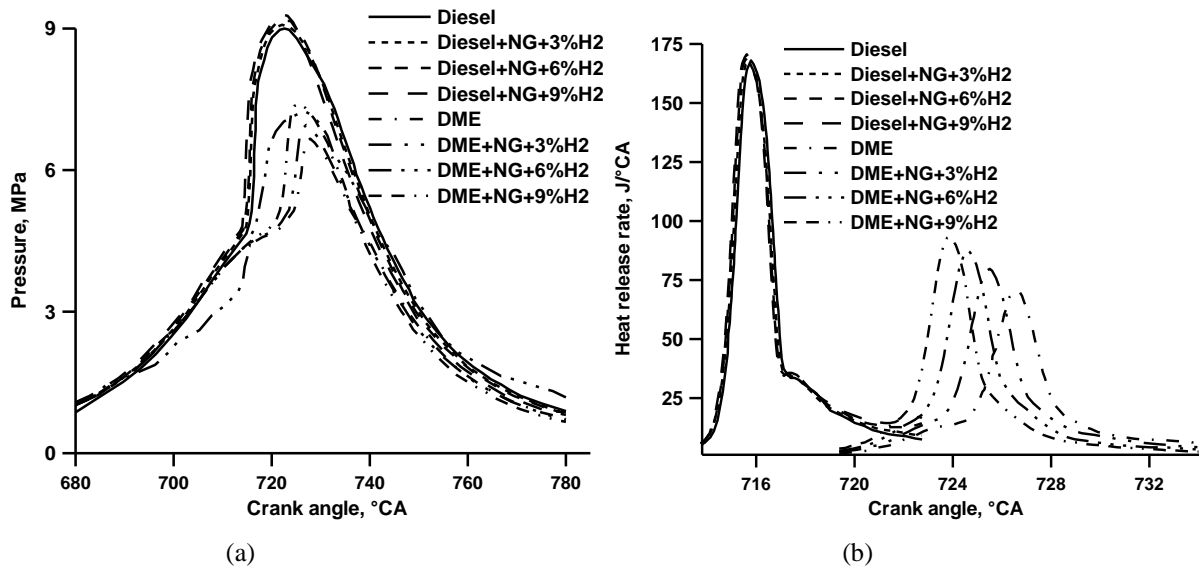
(a)   (b)

Figure 17. *Variation of a) pressure and b) heat release rate for Diesel–NG–H2 and DME–NG–H2 blends [82]*

Fig. 17(a) displays the combustion pressure for the hydrogen (H2) addition to NG–Diesel and NG–DME cases, from which it is clear that the NG–DME mixture is more sensitive against the addition of hydrogen; the increases in pressure for the NG–DME and NG–Diesel cases being 11.1% and 2.8%, respectively. According to this study, the maximum temperature showed the advancement with the addition of hydrogen for both NG–DME and NG–Diesel mixtures. This advancement was also noted in the pressure of all cases, as seen in Fig. 19(a). The cylinder temperatures of diesel and DME cases displayed a different behavior against the addition of hydrogen as an enhancer additive. The addition of hydrogen was found to have a greater influence on the cylinder temperature in DME cases, however, all temperatures in diesel cases were observed to be higher than the same case in NG–DME fuel mixtures. These results are also represented in the heat release rate diagram in Fig. 19(b), where the addition of hydrogen resulted in advancement in the start of combustion (SOC). Fig. 17(b) shows the heat release rate for various hydrogen additions to the NG–Diesel and NG–DME fuels. It

is evident from the figure that adding hydrogen has a different effect on the NG–DME fuel mixture in comparison to the NG–Diesel. As discussed, hydrogen addition is more effective on the NG–DME fuel mixture, which is also seen in the HRR diagrams. There are two different behaviors against the addition of hydrogen with respect to the maximum cumulative heat release (CHR). Hydrogen has a greater effect on the NG–DME fuel mixture, with the maximum CHR increasing by about 7.6% for a 9% addition to the fuel mixture. This process is different for the NG–Diesel mixture, with the trend of increasing maximum CHR decreasing as hydrogen is added. In each case, the CHR of NG–Diesel is higher than that of NG–DME, by 31%, 27%, 24%, and 22% respectively. These differences show the higher effect of hydrogen on the NG–DME fuel mixture, reducing the difference in combustion quality between NG–Diesel and NG–DME; the decrease in combustion quality with the use of DME is due to the in–cylinder behavior of DME, which breaks up into CH4, CO and H2 [82].

(a)   (b)
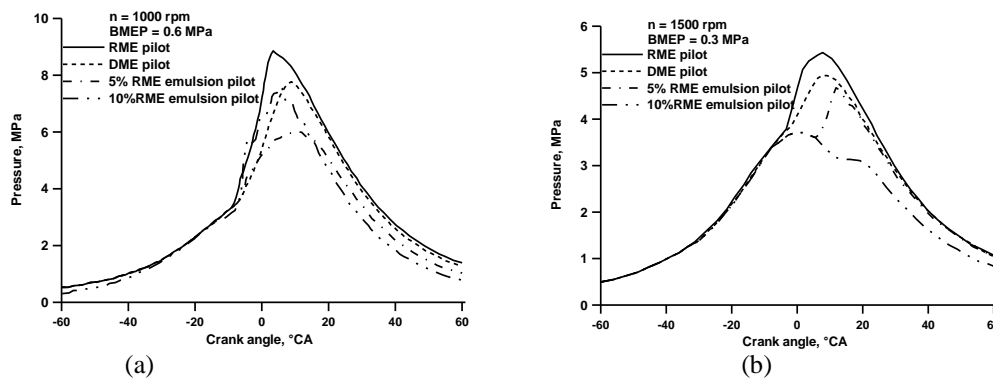
Figure 18. *Variation of pressure at a) 1000 rpm and 0.6 MPa and b) 1500 rpm and 0.3 MPa conditions for various pilot injection fuels in dual fuel natural gas engine [39]*

Fig. 18(a) shows the variation of pressure for all tested pilot fuels at 1000 rpm and BMEP of 0.6 MPa. It is observed that the 10% emulsion pilot and DME pilot fuel have similar peak pressure levels, but the peak of the DME occurs about 3.5° CA later than that of the 10% emulsified pilot. It is probable that the slightly extended ignition delay and comparatively slower rate of combustion of the DME pilot fuel are responsible for this retardation. Meanwhile, both emulsion pilot fuels and DME pilot produce lower peak pressures than the rapeseed–oil methyl ester (RME) pilot. For the emulsion pilot fuels, this is likely due to the cooling effect caused by the water vaporizing in the pilot fuel mixture, while the low combustion enthalpy of DME can explain its lower peak value. It is also noted that the rate of pressure rise for the 10% emulsion is highest in comparison with the other pilot fuels. This can be attributed to the micro explosion phenomenon occurring on a larger scale than the 5% emulsion, resulting in a better distribution of fuel across the combustion chamber. This would enable ignition to take place in more areas, accelerating combustion. This could be because the 5% emulsion does not contain enough water suspended in the atomized droplets, which impedes the number and intensity of micro explosions. The ignition delay of RME was the shortest (2.3 ms, while ignition started at 10.7° BTDC), followed by the 10% emulsion pilot fuel (2.6 ms, with ignition starting at 8.9° BTDC), then the 5% emulsion pilot fuel (2.7 ms, with ignition starting at 8.3° BTDC), and finally the DME pilot fuel (2.8 ms, with ignition starting at 7.7° BTDC). The emulsification of RME extended the pilot fuel's ignition delay by roughly 10–15% in comparison to neat RME at this engine speed. This can be attributed to the DME's higher auto–ignition temperature and its evaporation during injection, which would cool the charge mixture. Furthermore, with increasing natural gas flow rate, the mass flow rate of the emulsion pilot fuels slightly increased while the mass flow rate of DME was consistently greater than the other liquid pilot fuels due to its comparatively lower combustion enthalpy. Fig. 18(b) shows the pressure crank angle data for all pilot fuels at 1500 rpm and a BMEP of 0.3 MPa. Neat RME has the highest peak pressure, followed by the DME pilot and then the 5% emulsified pilot fuel, with the 10% emulsified pilot fuel having the lowest peak pressure. At this speed and load

condition, DME has a shorter ignition delay (2.3 ms, ignition starting at 3.8° ATDC) than the neat RME pilot (2.1 ms, starting at 5.6° ATDC). The 5% emulsified pilot fuel follows with an ignition delay of 3.3 ms (starting at 5.2° ATDC), and the 10% emulsified pilot fuel has the longest ignition delay at 3.8 ms (starting at 9.7° ATDC). It seems that the comparatively low combustion temperatures for dual–fuelling at this engine speed and load make it difficult for the micro explosion phenomenon to manifest. The higher concentration of water in the 10% emulsion appears to significantly impede combustion, which explains why the 5% and 10% emulsified pilot fuels reversed places compared to 1000 rpm. Different trends at 1000 and 1500 rpm may be attributed to the quality of emulsions. Before reaching the engine, the emulsions and neat RME were mixed in the emulsifying circuit and then entered a fuel measuring flask. As the engine consumed the fuel, it stayed undisturbed in the flask, downstream of which was a fuel line of about 60 cm in length, after which the emulsions went into the engine's fuel system. This fuel line contained water during operation, so there was a risk that the injected volume of emulsion did not contain the necessary amount of water. RME and DME pilots both account for about 40% of combustion enthalpy, whereas emulsions provide only about 34%. The higher mass flow rate of DME participating in combustion can explain its relatively short ignition delay at this engine speed. Furthermore, at the highest natural gas flow rate corresponding to this condition, the mass flow rate of the emulsified pilot fuels decreases slightly compared to lower load conditions. It is clear that the mass flow rate of DME is consistently higher than the liquid pilot fuels. At 1500 rpm, the amount of natural gas inducted per cycle is lower than at 1000 rpm. This is because the flow rate of natural gas is held constant for both engine speeds while entering the engine intake manifold. As a result, the reduced amount of natural gas coupled with the cooling effect of the emulsified pilot fuels leads to noticeably lower and significantly delayed peak pressures. Furthermore, the engine was stalling at high load in dual–fuel mode when using the emulsified pilot fuel. This was because the emulsion was separating in the fuel line. Due to these factors, the same load ranges visible at 1000 rpm couldn't be reproduced [39].
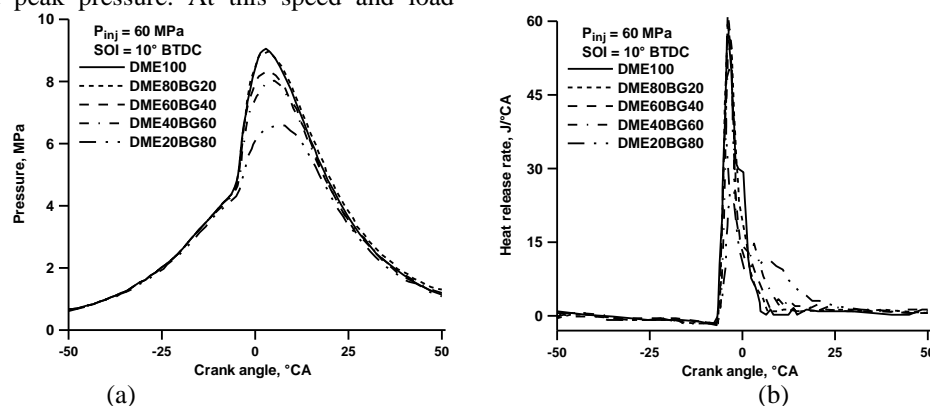

Figure 19. *Variation of a) pressure and b) heat release rate for DME–BG (biogas) blends [75]*

Fig. 19(a) and (b) shows the combustion pressure and heat release rate characteristics for different DME–biogas (BG) blends in DME–fueled diesel engines with common–rail injection systems, compared in the range of injection timing from 10° BTDC to 40° BTDC with an interval of 10° CA. It can be seen from Fig. 19(a) that the peak combustion pressure tended to decrease with increasing mixing ratio of biogas at the same injection timing. The test fuel with biogas ratio of 0.2 still had so much DME compared to pure DME combustion, so it showed a similar pressure trajectory with DME. However, higher mixing ratio conditions (biogas ratio of 0.8) showed different combustion behavior, especially at BTDC 40°, where misfire occurs. At the same injection timing, the increase in mixing ratio of biogas caused an increase in the coefficient of variation for the peak combustion pressure, retardation of ignition timing, and a decrease in the rate of combustion pressure increase. An advance in injection timing induced a visible trajectory of combustion pressure according to changes in the mixing ratio of biogas. The time difference to reach the same combustion pressure increased with an advance in the injection timing between DME and a higher mixing ratio fuel with a biogas ratio of 0.6, as shown in the pressure diagram of Fig. 19(a). For example, at an injection timing of 10° BTDC, 0.3 degree difference was observed between DME and biogas ratio of 0.6 test fuels to reach 6 MPa combustion pressure. Whereas, at 40° BTDC, 30° BTDC, and 20° BTDC, an increase to 7.5, 5.5, and 1.4 degrees was required, respectively. In this case, it is important to understand why the distribution of DME as an ignition source in the combustion chamber changed as the injection timing was advanced. When the injection timing was close to TDC, the injected DME spray was mainly distributed in the piston bowl. Thus, the injected DME mixed with the biogas that flowed into the combustion chamber through the intake port. In addition, this mixture of biogas and DME can react with the oxygen in the combustion chamber for ignition and combustion. However, when DME fuel is injected from 30° BTDC to 40° BTDC into crevice and squish regions, the ignition and combustion are less active due to low utilization of oxygen. On the other hand, when the biogas ratio is 0.8, composed of 80% intake biogas and 20% direct injection DME, the ignition and combustion characteristics are found to be unstable. Thus, it is determined that the biogas ratio of 0.8 is not suitable [75].

Fig. 20(a) and (b) compare cylinder pressure and heat release rate data for DME–NH3 blends. The injection timings are 10°, 20°, and 18° BTDC for 100%DME, 60%DME–40%NH3, and 40%DME–60%NH3, respectively. As shown in Fig. 22(a), the cylinder pressure history of 40%DME–60%NH3 is distinct from those of 100%DME and 60%DME–40%NH3. The pressure trace of 40%DME–60%NH3 is slightly higher during the compression process, and lower during the expansion process, despite the heat release rate indicating no combustion before TDC. 100%DME exhibits diesel combustion with its premixed combustion, mixing–controlled combustion, and late combustion phases identified in conventional compression ignition engines and its ignition delay is 4° CA. For 60%DME–40%NH3, a longer ignition delay of 19.5° CA is observed; causing a very significant premixed combustion and a late combustion phase is visible from the heat release rate data. With very early injection timing, 40%DME–60%NH3 has a homogeneous combustion phase with short combustion duration, like that seen in HCCI combustion. It is assumed that the early injection of 40%DME–60%NH3 causes complete evaporation of the fuel during the intake and compression process, causing the rise of pressure in the cylinder due to the increase of vapor pressure. This early injection also gives the fuel and air enough time to mix completely, resulting in homogeneous combustion. However, 100%DME and 60%DME–40%NH3 demonstrate typical diesel combustion and maintain higher cylinder pressure during the expansion process compared to 40%DME–60%NH3, due to its lower combustion temperature, which reduces the pressure in the expansion stroke. Fig. 20(c) shows the cumulative heat release fraction (i.e., mass burn fraction) corresponding to the conditions in Fig. 20(c). It can be seen that combustion of 100%DME steadily advances until 140° ATDC, indicating slow diffusion combustion during the later stage. On the other hand, 60%DME–40%NH3 has 90% heat release within 40° CA after ignition and continues to release heat through 70° ATDC, exhibiting greater premixed combustion phase and smaller mixing controlled combustion phase, similar to PCCI. Lastly, 40%DME–60%NH3 has extremely short combustion duration of 20° CA, which is attributed to the early fuel injection timing and indicates HCCI combustion [41].
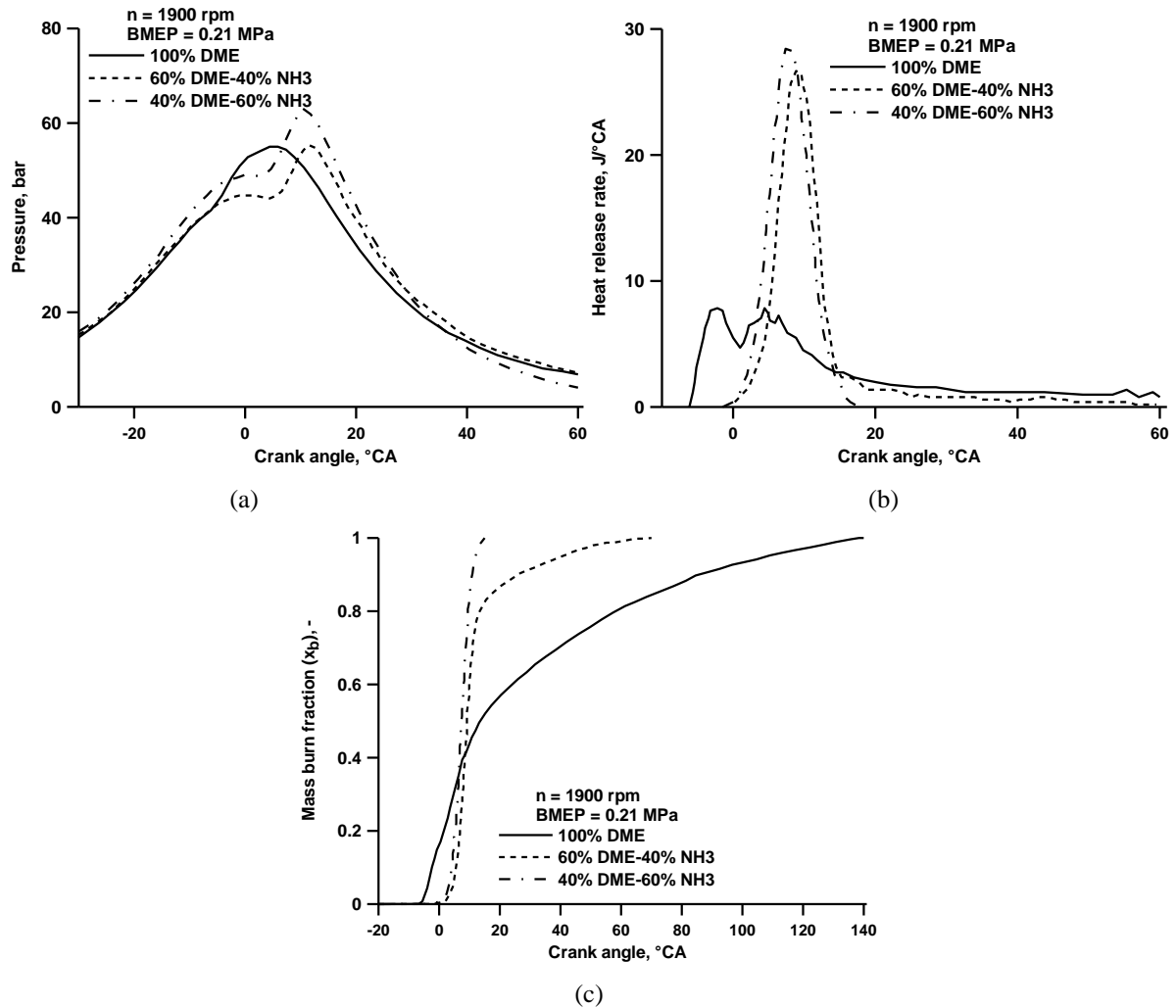
(a)

(b)

(c)

Figure 20. *Variation of a) pressure, b) heat release rate and c) mass burn fraction for DME–NH3 blends [41]*

Fig. 21 shows the combustion pressure and pressure rise rate at various crank angles for injection timing of 20° BTDC. As shown in Fig. 21(a), the motoring combustion pressure before injection timing of 20° BTDC decreases with increasing ethanol fraction. This decrease is due to heat absorption by ethanol evaporation. The polytrophic index calculated for the test conditions of 100% DME was about 1.26, whereas the DME–ethanol dual–fuel cases had lower values of 1.23–1.25. Generally, the polytrophic index for adiabatic compression of air is 1.4, and lower values are the result of heat loss to the cylinder walls or the heat absorbed by fuel vaporization. Hence, it is assumed that ethanol evaporation induced the lower motoring combustion pressure before injection. After injection, the ignition timing was retarded as the ethanol fraction increased; consequently, the ignition delay was prolonged. This increase in the ignition delay with increasing ethanol fraction caused an increase of the combustion pressure rising rate. Thus, the PRR increased with increasing ethanol fraction, as shown in Fig. 21(b) [61].
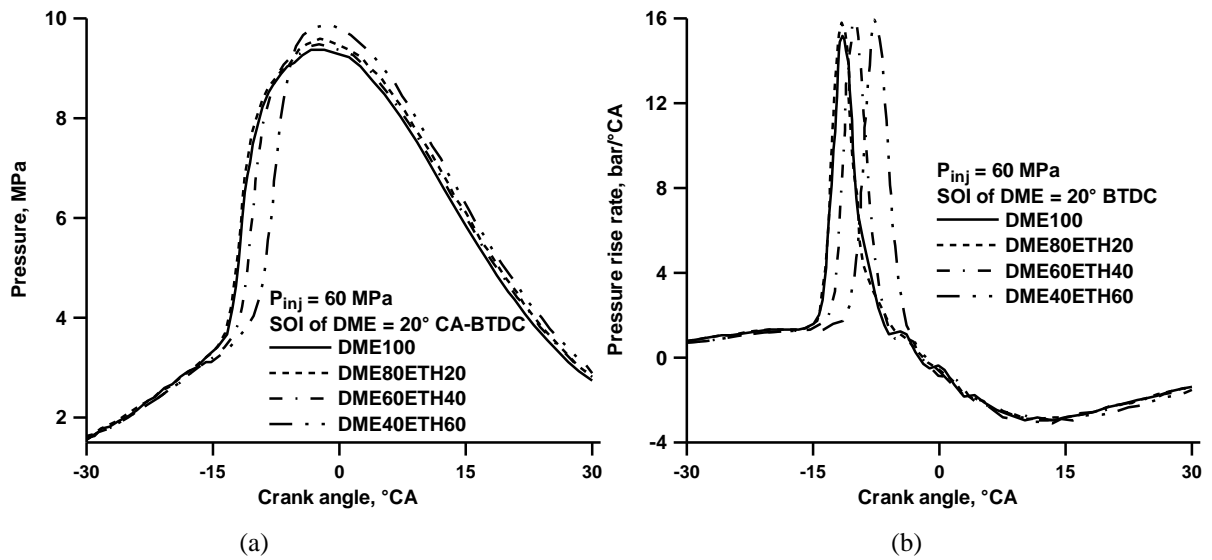
(a)   (b)

Figure 21. *Variation of a) pressure and b) heat release rate for DME–ethanol (ETH) blends [61]*

Fig. 22 shows the cylinder pressure, heat release rate, cylinder temperatures, and pressure rise rate at 1.52 MPa brake mean effective pressure (BMEP). With the increase of DME proportion, the peak pressure decreases and its phase retards as seen in Fig. 22(a). The cylinder pressure peaks are 12.5 MPa at 14.5° ATDC, 11.7 MPa at 14.5° ATDC, 10.9 MPa at 16° ATDC, and 10.1 MPa at 1.5° BTDC. The cetane number of biodiesel is lower than DME, resulting in a longer ignition delay period and more fuel accumulation in the cylinder during this delay. Therefore, the maximum pressure of Biodiesel, DME50, DME70, and DME100 progressively

decrease. It is clear that the combustion of DME–biodiesel blends shows the diffusion combustion mode without premixed combustion. The pressure rise rate decreases and its phase are retarded with the increasing DME proportion as seen in Fig. 24(b). The pressure rise rate reflects the combustion rate and heat release rate; thereby, a larger pressure rise rate implies a cruder engine operation. Accordingly, DME blending can ensure a more stable engine operation. The intake air temperature and pressure of a turbocharged engine are higher at full load, thus resulting in a shorter ignition delay [25].
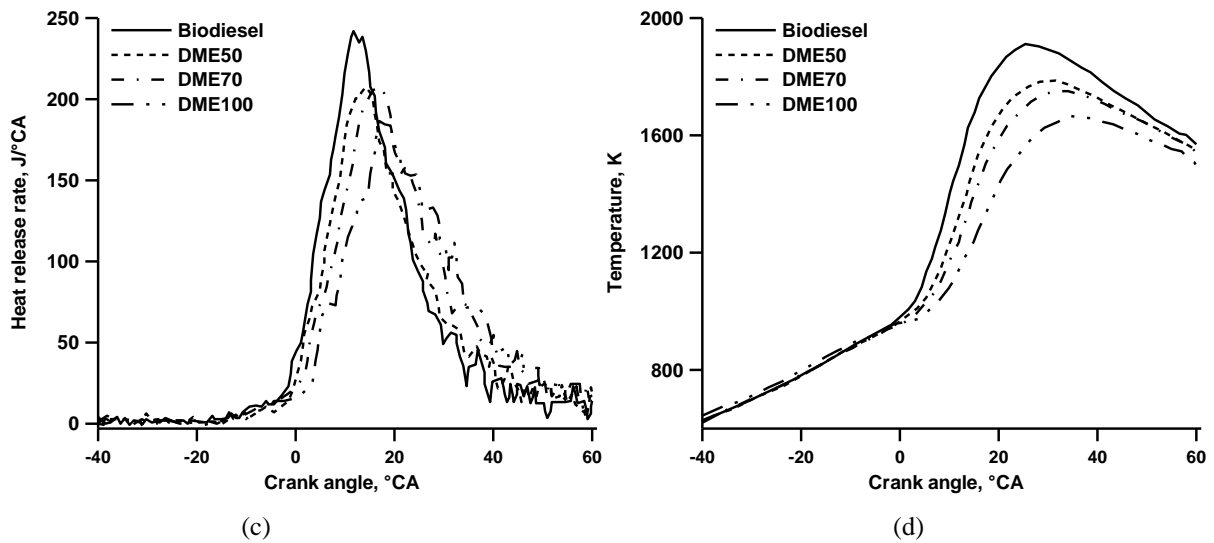

(a)   (b)
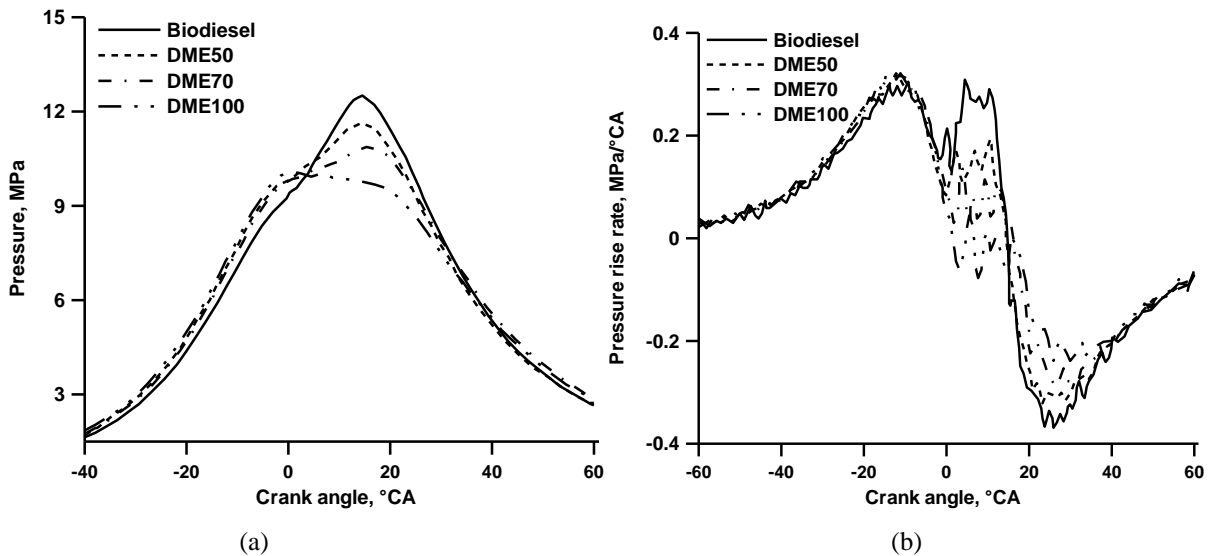
Figure 22. *Variation of a) pressure, b) pressure rise rate, c) heat release rate and d) temperature for biodiesel–DME blends [65]*

As seen in Fig 22(c), the ignition timing retards, and the peak heat release rate decreases while its phase retards with the increase of the DME proportion. Specifically, the peak heat release rate of biodiesel, DME50, DME70, and DME100 are respectively 241.9 J/°CA at 11.5° ATDC, 210.7J/°CA at 12.5° ATDC, 208.8 J/°CA at 17° ATDC, and 186.9 J/°CA at 19° ATDC. Although the cetane number of DME is higher than that of biodiesel, its ignition delay is shorter due to its lower propagation velocity of fuel pressure wave in the pipe and longer fuel injection delay. Consequently, the peak heat

release rate drops and its phase retards. With the increase of DME proportion, the peak cylinder temperature decreases and its phase is delayed as seen in Fig. 22(d). The peak cylinder temperature of biodiesel, DME50, DME70 and DME100 are 2097 K, 1954 K, 1914 K, and 1838 K, respectively, and the corresponding phases are 26° CA, 30.5° CA, 32.5° CA and 39.5° CA. The later ignition and combustion is attributed to the higher latent heat of vaporization of DME compared to biodiesel, which leads to more heat absorption during vaporization [65].
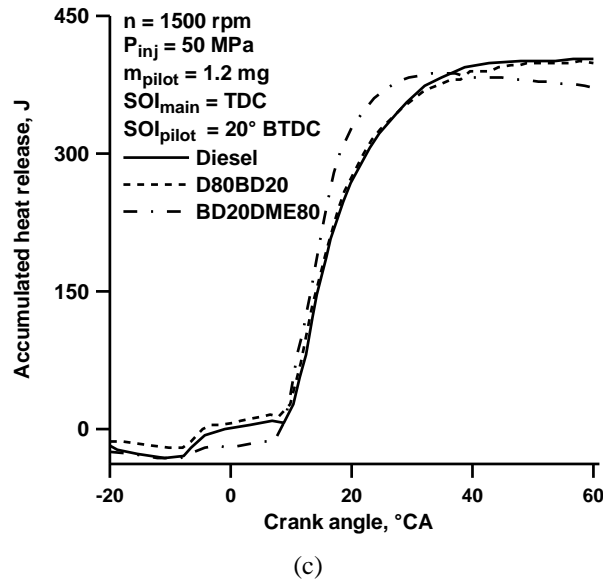
(c)
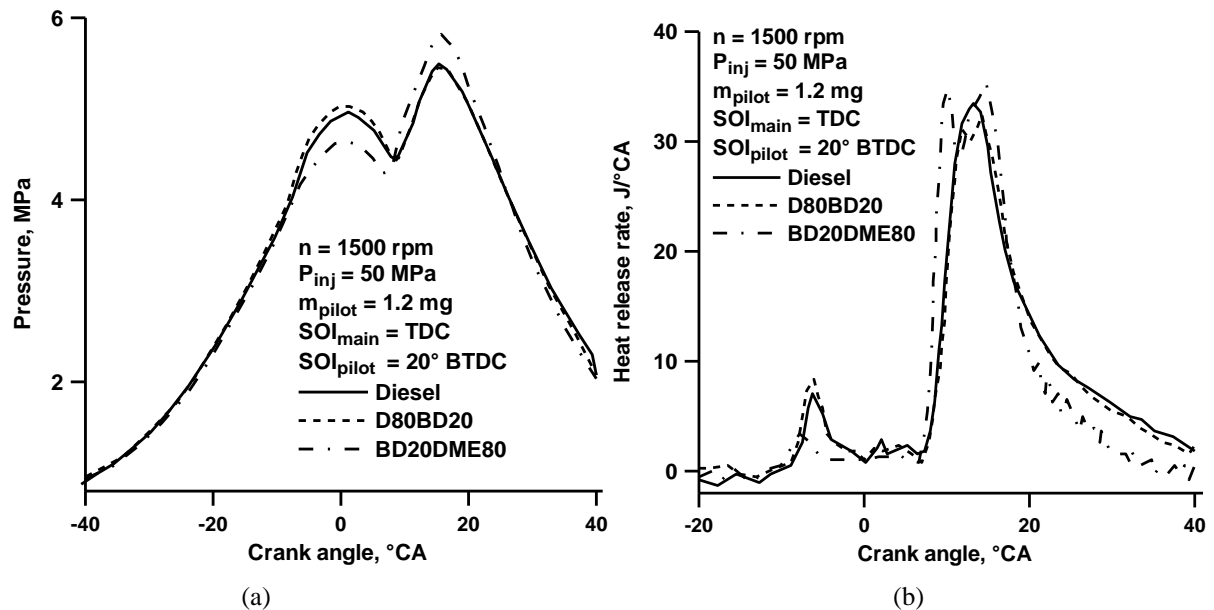
Figure 23. *Variation of a) pressure, b) heat release rate and c) accumulated heat release for diesel–biodiesel–DME blends [73]*

Fig. 23 shows the effect of *DME*–biodiesel blend (DME80BD20), diesel–biodiesel blend (D80BD20), and diesel (D), on the combustion pressure, heat release rate, and accumulated heat release in a CI engine at 1500 rpm with various pilot injection timings. The combustion characteristics were investigated with a fuel injection pressure of 50 MPa, pilot injection quantity of 1.2 mg, and a main injection timing of top dead center (TDC) [73]. As illustrated in Fig. 23(a), the DME–biodiesel blend (DME80BD20) had a higher peak pressure than that of the diesel–biodiesel blend (D80BD20) and conventional diesel fuel. This could be attributed to the lower bulk modulus of DME fuel than conventional diesel fuel at the same temperature in a closed system. Thus, the higher compressibility and low heating value of DME required higher energy input and fuel quantity than that of diesel fuel, resulting in a higher peak pressure at a constant engine load.

The pressure rise near TDC is similar for diesel and D80BD20 fuels, while DME80BD20 blend exhibited lower values than that of the other fuels; primarily due to its low lower heating value (LHV). The LHV of DME80BD20 is 29.92 MJ/kg, and those of diesel and D80BD20 fuel are 42.5 MJ/kg and 41.83 MJ/kg, respectively. For the same injection quantity, a lower peak from the DME–biodiesel blend combustion was observed because of the relatively low LHV of DME. On the other hand, the heat release rate of DME80BD20 indicates that heat release in the pilot injection occurred at approximately 10° BTDC. The heat release of the main injection showed the advanced burning of DME80BD20 fuel when compared to diesel and D80BD20 fuel. Thus, the conventional diesel and diesel–biodiesel blend (D80BD20) resulted in higher pressure at the TDC region, while the DME80BD20 fuel exhibited lower pressure than D80BD20 [73].

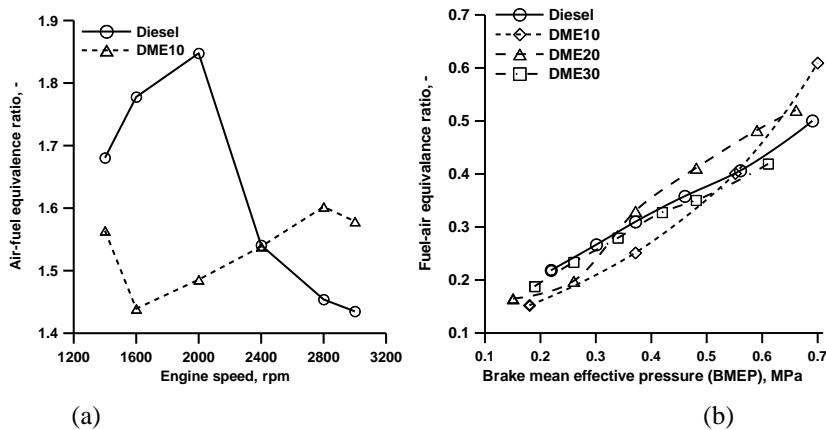## 6. Effects of dimethyl ether on air–fuel ratio

(a)   (b)

Figure 24. *Variation of air–fuel equivalence ratio for DME blend a) [55] and b) [66]*

Fig. 24(a) compares the air–fuel equivalence ratio of diesel (D) and DME10 blend. It can be seen from the figure that the air–fuel ratio of DME10 blend is lower at low engine speed and higher at high engine speeds than diesel fuel. This is due to the higher amount of fuel delivery for higher output torque at low engine speeds and the lower amount of fuel injection by decreasing engine load at high engine speeds. As a result of this, the lower air–fuel ratio is obtained with DME10 blend at low engine speeds [55]. It is also seen from Fig. 24(b) the DME10 blend has lower fuel–air equivalence ratio than those of diesel fuel, DME20 and DME30blends, especially at low engine loads [66].

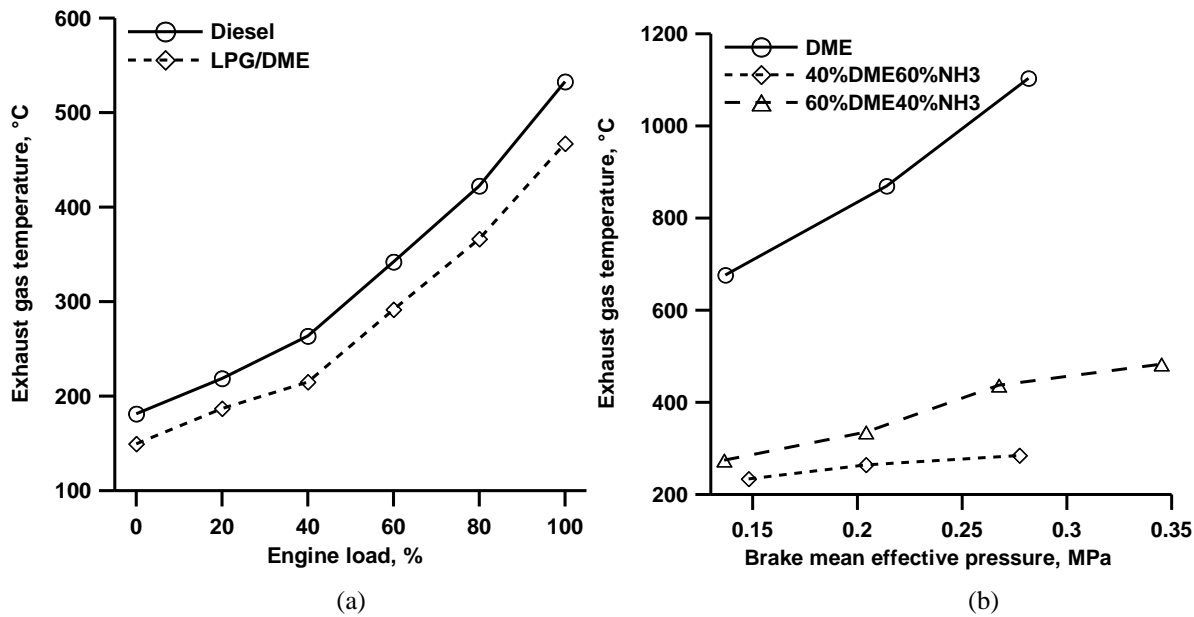## 7. Effects of dimethyl ether on exhaust gas temperature

Figure 25. *Variation of exhaust gas temperature for a) Diesel and LPG–DME blend [24] and b) DME and DME–NH₃ blends [41]*

Fig. 25(a) depicts the variation of exhaust gas temperature (EGT) under different engine loads. It can be seen from the Fig. 25(a) that EGT is found to be lower by about 40–50 °C in the case of LPG–DME operation throughout the load spectrum as compared to diesel operation. It is declared that the higher latent heat of vaporization of DME cools the intake charge, which reduces the peak temperature of the combustion in the engine cylinder and also EGT [24]. Fig. 25(b) shows the comparison of EGT versus brake mean effective pressure (BMEP). It is seen in the figure that EGT values for 100% DME are higher than those for both 60%DME–40%NH₃ and 40%DME–60%NH₃ blends. It is noted that EGT decreases as the ammonia (NH₃) concentration is increased in the blend. It is commended that the reduction in EGT is due to the loss in energy of the combustion process caused by the high latent heat of ammonia. It also stated that this is especially evident in case of 40%DME–60%NH₃ blend where the fuel charge has sufficient time to fully evaporate, drawing the full latent heat energy out of the in–cylinder air [41].
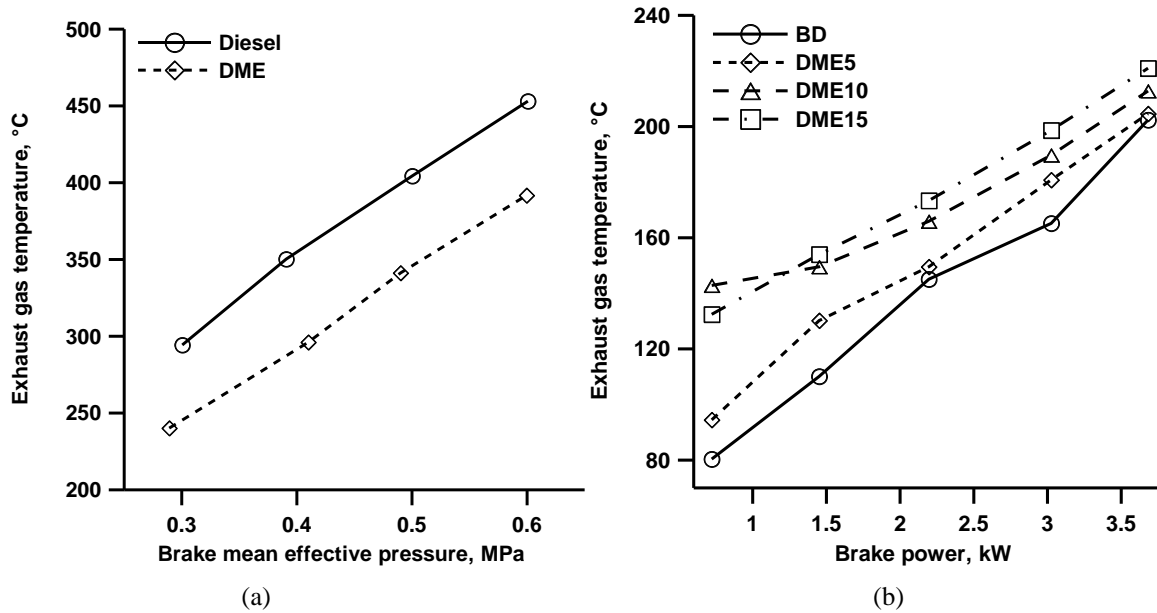
(a)   (b)

Figure 26. *Variation of exhaust gas temperature for a) Diesel and DME [54] and b) Biodiesel and Biodiesel–DME blends [63]*

Fig. 26(a) shows a comparison of the EGT between DME and diesel fuel. The exhaust gas temperature is plotted against brake mean effective pressure (BMEP). It seen from the Fig. 26(a) that EGT is lower for DME by around 50 °C compared to diesel fuel. It is declared that the reason of this reduction in EGT is the lower energy content of DME [54]. Fig. 28(b) illustrates that EGT for the biodiesel (BD) and its blends with DME namely DME5, DME10 and DME15. It is seen from the Fig. 26(b), EGT are increased for all the fuels with the increase of engine load and DME blends give the higher EGT values

than BD fuel. Additionally, EGT increases with the increase of DME ratio so DME15 blend gives higher EGT values than DME5 and DME10 blends at all engine loads. It is declared that increases in EGT when using of DME blends is sourced from the enhanced combustion due the higher oxygen content and the other fuel properties improved the combustion of DME. It is also stated that another reason for increase of EGT may be the shortened combustion period because of the higher flame velocity of DME [63].

8.   Effects of dimethyl ether on CO_2 emissions

Fig. 27(a) illustrates the NOx and CO_2 emissions for DME compared with diesel fuel from a six–cylinder turbocharged–intercooler heavy–duty diesel engine operating in the Japanese JE–05 test mode. It is seen from the figure that DME provides the significant reduction in CO_2 emissions compared to diesel fuel. It is also declared the reduction in NOx and CO_2 emissions that can be achieved with DME at a similar fuel economy. It is stated that CO_2 emissions is about 10% less

than that of diesel fuel when using DME due to based on the difference between the C/H ratio of fuels [56]. Fig. 27(b) gives the CO_2 emissions characteristics when DME10 and DME20 blends are used. It is seen the figure that compared to diesel fuel there is obvious reduction in CO_2 emissions for DME10 and DME20 blends at most BMEP values. It is declared that the possible reason of this reduction in CO_2 emissions is the low C/H ratio and oxygen content of the DME blends [34].
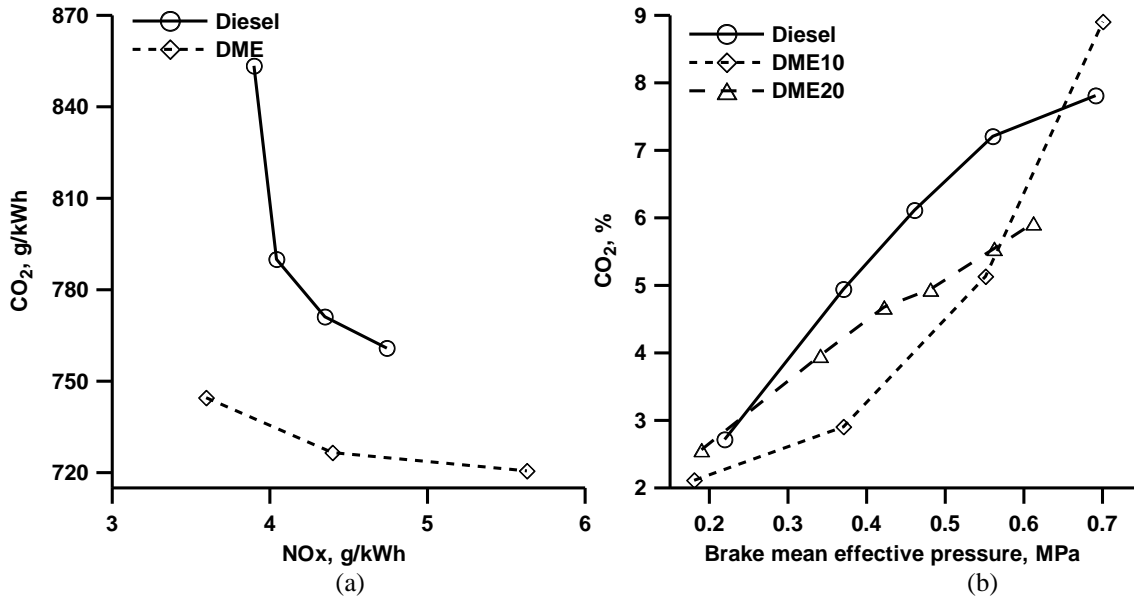
Figure 27. *a) Variation of CO_2 emissions for a) Diesel and DME [56] and b) Diesel and Diesel–DME blends [34]*
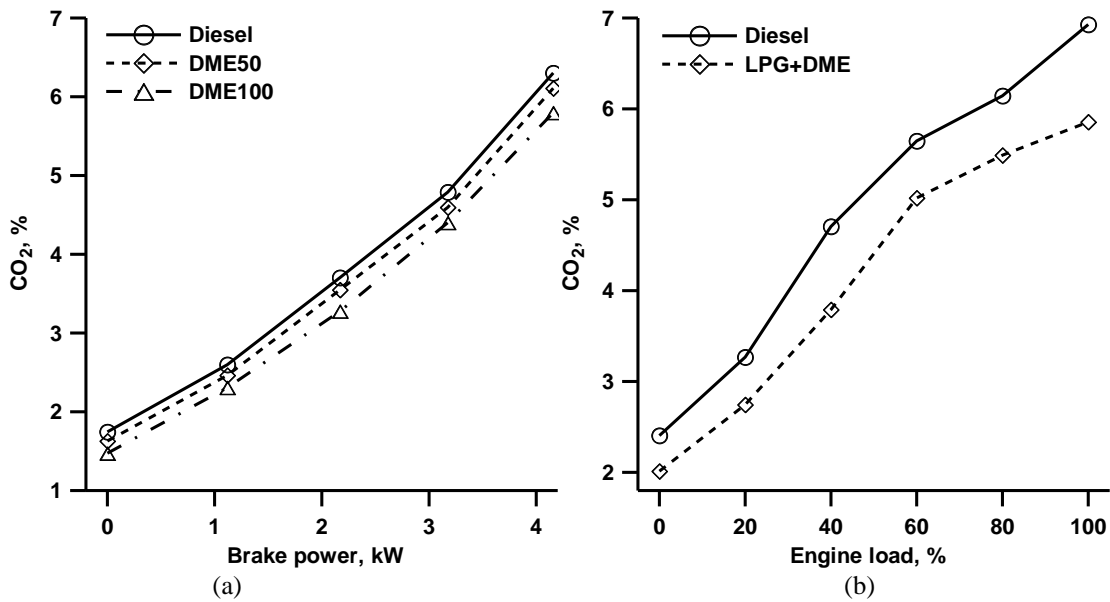
Figure 28. *Variation of CO_2 emissions for a) Diesel and Diesel–DME blend [53] and b) Diesel and LPG–DME blend [24]*

It can be also observed from Fig. 28(a) that CO_2 emissions are lower for pure DME (DME100) and DME50 blend than diesel fuel because of the same reasons [53]. The variation of CO_2 emissions levels for diesel fuel and LPG–DME blend at different loads is shown in Fig. 28(b). It is seen from the figure that CO_2 emission level is lower for LPG–DME blend compared to diesel fuel. It is explained that the reduction in CO_2 emissions due to lower carbon to hydrogen ratio of DME compared to LPG [24].

Table 2. The variations in the results obtained with using of DME

Base Fuel–Blend	Reference	Air–Fuel Ratio	EGT	CO_2 Emissions
		Variation (%)		
D–LPG+DMEX	[24]	–	↓12–18.3	↓10.6–19.4
D–DME10	[34]	–	–	↓41.6– ↑14.1
D–DME20	[34]	–	–	↓5.8–31.8
DME–40DME60NH3	[41]	–	↓60.2–61.8	–
DME–60DME40NH3	[41]	–	↓65.6–69.8	–
D–DME50	[53]	–	–	↓3–7.7
D–DME100	[53]	–	–	↓8.5–18.3
D–DME100	[54]	–	↓13.6–18.6	–
D–DME10	[55]	↓19.6– ↑10.2	–	–
D–DME100	[56]	–	–	↓5.2–5.7
BD–DME5	[63]	–	↑1.7–17.3	–
BD–DME10	[63]	–	↑4.9–70.8	–
BD–DME15	[63]	–	↑9–59	–
D–DME10	[66]	↓30.2– ↑21.8	–	–
D–DME20	[66]	↓25.7– ↑18.7	–	–
D–DME30	[66]	↓8.5–16.2	–	–

9. Conclusions

The effects the use of dimethyl ether on CO_2 emissions in diesel engines are examined in this review study. The following conclusions can be summarized as obtained findings of the study.

- The use of dimethyl ether significantly affected the combustion characteristics such as pressure, temperature and heat release in diesel engines. The use of pure dimethyl ether caused to decreases in the combustion characteristics at the same amount of fuel input, while the combustion characteristics were improved with increased dimethyl ether fuel at the same amount of energy input compared diesel fuel. The use of dimethyl ether together with the liquid fuels such as diesel, biodiesel and ethanol generally improved the combustion characteristics, while the combustion characteristics can be adversely affected when the use of dimethyl ether together with the gaseous fuels such as LPG, natural gas, biogas and hydrogen. However, the negative changes in combustion characteristics are quite low and do not prevent the use of dimethyl ether.

- Air–fuel equivalence ratio decreases when using the diesel–DME blend, especially at low engine speeds, providing high engine torque, because of the lower stoichiometric air–fuel ratio of DME. However, air–fuel equivalence ratio increases when using the diesel–DME blend at high engine speeds and loads because of the increased fuel injection. The decrement in air–fuel equivalence ratio for DME10 blend is about 30.2%, while the increment is about 21.8%.

- Exhaust gas temperature decreases when using the pure DME and its blends with diesel, LPG and NH_3 fuels due to lower heating value of DME, while DME and its blends with biodiesel gives the higher exhaust gas temperature than biodiesel due to enhanced combustion. The decrements in exhaust gas temperature for pure DME, diesel–DME blends, LPG–DME blend and DME–NH_3 blends are about 13.6–18.6%, 12–18.3% and 60.2–69.8%, respectively, while the increments for biodiesel–DME blends are about 1.7–59%.

- CO_2 emissions decrease when using the pure DME and DME blends with diesel and LPG fuels due to the oxygen

content and the lower carbon to hydrogen ratio of DME. The decrements in CO_2 emissions for pure DME, diesel–DME blends and LPG–DME blend are about 5.2–18.3%, 3–41.6% and 10.6–16.4%, respectively.

References

[1]. Yoon SH, Cha JP Lee CS. An investigation of the effects of spray angle and injection strategy on dimethyl ether (DME) combustion and exhaust emission characteristics in a common–rail diesel engine. Fuel Processing Technology 2010; 91: 1364–1372.

[2]. Youn IM, Park SH, Roh HG, Lee CS. Investigation on the fuel spray and emission reduction characteristics for dimethyl ether (DME) fueled multi–cylinder diesel engine with common–rail injection system. Fuel Processing Technology 2011; 92: 1280–1287.

[3]. Alam M, Kajitani S. DME as an alternative fuel for direct injection diesel engine. 4th International Conference on Mechanical Engineering 2001; 87–92.

[4]. Maji S, Ahmed S, Siddiqui WA, Kumar A. Impact of di–methyl ether (DME) as an additive fuel for compression ignition engine in reduction of urban air pollution. International Journal of Innovative Research in Science, Engineering and Technology 2014; 3(11): 17221–17228.

[5]. Park SH, Lee CS. Applicability of dimethyl ether (DME) in a compression ignition engine as an alternative fuel. Energy Conversion and Management 2014; 86: 848–863.

[6]. Wattanavichien K. Implementation of DME in a small direct injection diesel engine. International Journal of Renewable Energy 2009; 4(2): 1–12.

[7]. Duan J, Sun Y, Yang Z, Sun Z. Combustion and emissions characteristics of diesel engine operating on composite combustion mode of DME and diesel. Proceedings of International Conference on Mechanical Engineering and Material Science 2012; 27: 463–466.

[8]. Kowalewicz A, Wojtyniak M. Alternative fuels and their application to combustion engines. Journal of Automobile Engineering 2005; 219: 103–125.

[9]. Azizi Z, Rezaeimanesh M, Tohidian T, Rahimpour MR. Dimethyl ether: A review of technologies and production challenges. Chemical Engineering and Processing 2014; 82: 150–172.

[10]. Huang Z, Qiao X, Zhang W, Wu J, Zhang J. Dimethyl ether as alternative fuel for CI engine and vehicle. Frontiers of Energy and Power Engineering in China 2009; 3(1): 99–108.

[11]. Lecksiwilai N, Gheewala SH, Sagisaka M, Yamaguchi K. Net energy ratio and life cycle greenhouse gases (GHG) assessment of bio–dimethyl ether (DME) produced from various agricultural residues in Thailand. Journal of Cleaner Production 2016; 134: 523–531.

[12]. Inayat A, Ghenai C, Naqvi M, Ammar M, Ayoub M, Hussin MNB. Parametric study for production of dimethyl ether (DME) as a fuel from palm wastes. Energy Procedia 2017; 105: 1242–1249.

[13]. Park SH, Lee CS. Combustion performance and emission reduction characteristics of automotive DME engine system," Progress in Energy and Combustion Science 2013; 39: 147–168.

[14]. Teng H, McCandless JC, Jeffrey BS. Thermochemical characteristics of dimethyl ether alternative fuel for compression–ignition. Society of Automotive Engineers 2001; Paper no 2001–01–0154.

[15]. Maji S, Ahmed S, Siddiqui WA, Aggarwal S, Kumar A. Impact of di–methyl ether (DME) as an additive fuel for compression ignition engine in reduction of urban air pollution. American Journal of Environmental Protection 2015; 3(2): 48–52.

[16]. Guangxin G, Zhulin Y, Apeng Z, Shenghua L, Yanju W. Effects of fuel temperature on injection process and combustion of dimethyl ether engine. Journal of Energy Resources Technology 2013; 135: 1–5.

[17]. Jalanapurkar M, Patel K, Patel T, Rathod G, Granipa H. A literature review on combine effect of di–methyl ether (DME) as an additive & the injection pressure on the performance & emission of 4 stroke C.I engine. International Journal of Advance Engineering and Research Development 2015; 2(1): 262–266.

[18]. Kim HJ, Park SH, Lee KS, Lee CS. A study of spray strategies on improvement of engine performance and emissions reduction characteristics in a DME fueled diesel engine. Energy 2011; 36: 1802–1813.

[19]. Xu S, Wang Y, Zhang X, Zhen X, Tao C. Development of a novel common–rail type dimethyl ether (DME) injector. Applied Energy 2012; 94: 1–12.

[20]. Lim OT, Iida N. A study on the spray and engine combustion characteristics of diesel–dimethyl ether fuel blends. Journal of Automobile Engineering 2015; 229(6): 782–792.

[21]. Suh HK, Lee CS. Experimental and analytical study on the spray characteristics of dimethyl ether (DME) and diesel fuels within a common–rail injection system in a diesel engine. Fuel 2008; 87: 925–932.

[22]. Genbao L, Jianming C, Minglong L, Yuhua Q, Zhaoyang C. Experimental study on the size distribution

characteristics of spray droplets of DME/diesel blended fuels. Fuel Processing Technology 2012; 104: 352–355.

[23]. Mohan B, Yang W, Yu W, Tay KL. Numerical analysis of spray characteristics of dimethyl ether and diethyl ether fuel. Applied Energy 2017; 185: 1403–1410.

[24]. El–Hagar MME–G. Effect of diethyl ether and dimethyl ether with liquefied petroleum gas on combustion and emissions characteristics of diesel engine. International Journal of Computer Science and Engineering 2014; 2(3): 193–198.

[25]. Wang Y, Xiao F, Zhao Y, Li D, Lei X. Study on cycle–by–cycle variations in a diesel engine with dimethyl ether as port premixing fuel. Applied Energy 2015; 143: 58–70.

[26]. Jeon J, Kwon S, Park YH, Oh Y, Park S. Visualizations of combustion and fuel/air mixture formation processes in a single cylinder engine fueled with DME. Applied Energy 2014; 113: 294–301.

[27]. Baskaran R. Analysis on synthesis, storage & combustion characteristics of DME as fuel in CI engines. International Journal for Research in Applied Science & Engineering Technology 2015; 3(1): 133–140.

[28]. Park S. Optimization of combustion chamber geometry and engine operating conditions for compression ignition engines fueled with dimethyl ether. Fuel 2012; 97: 61–71.

[29]. Benajes J, Novella R, Pastor JM, Hernández–López A, Kokjohn SL. Computational optimization of the combustion system of a heavy duty direct injection diesel engine operating with dimethyl–ether. Fuel 2018; 218: 127–139.

[30]. Oda Y, Osafune Y, Ueda H, Fujimura K. Clean combustion technology in diesel engines operated with dimethyl ether. Mitsubishi Heavy Industries Ltd. Technical Review 2004; 40(6): 1–5.

[31]. Song J, Huang Z, Qiao X, Wang W. Performance of a controllable premixed combustion engine fueled with dimethyl ether. Energy Conversion and Management 2004; 45: 2223–2232.

[32]. Khunaphan S, Hartley UW, Theinnoi K. Characterization and potential of dimethyl ether (DME) as dual fuel combustion in a compression ignition engine. International Journal of Engineering Science and Innovative Technology 2013; 2(3): 79–85.

[33]. Lamani VT, Yadav AK, Narayanappa KG. Influence of low–temperature combustion and dimethyl ether–diesel blends on performance, combustion, and emission characteristics of common rail diesel engine: a CFD

study. Environmental Science and Pollution Research 2017; 24: 15500–15509.

[34]. Chapman EM, Boehman AL. Pilot ignited premixed combustion of dimethyl ether in a turbodiesel engine. Fuel Processing Technology 2008; 89: 1262–1271.

[35]. Ying W, Longbao Z, Zhongji Y, Hongyi D. Study on combustion and emission characteristics of a vehicle engine fuelled dimethyl ether. Journal of Automotive Engineering 2005; 219: 263–269.

[36]. Benajes J, Novella R, Pastor JM, Hernández–López A, Kokjohn S. Computational optimization of a combustion system for a stoichiometric DME fueled compression ignition engine. Fuel 2018; 223: 20–31.

[37]. Kropiwnicki J, Dominiczak P, Kneba Z. Analysis of the possibilities of using of DME fuel in motor boat drive systems. Combustion Engines 2017; 171(4): 74–80.

[38]. Smolec R, Idzior M, Karpiuk W, Kozak M. Assessment of the potential of dimethyl ether as an alternative fuel for compression ignition engines. Combustion Engines 2017; 169(2): 181–186.

[39]. Namasivayam AM, Korakianitis T, Crookes RJ, Bob–Manuel KDH, Olsen J. Biodiesel, emulsified biodiesel and dimethyl ether as pilot fuels for natural gas fuelled engines. Applied Energy 2010; 87: 769–778.

[40]. Jang J, Bae C. Effects of valve events on the engine efficiency in a homogeneous charge compression ignition engine fueled by dimethyl ether. Fuel 2009; 88: 1228–1234.

[41]. Ryu K, Zacharakis–Jutz GE, Kong S–C. Performance characteristics of compression– ignition engine using high concentration of ammonia mixed with dimethyl ether. Applied Energy 2014; 113: 488–499.

[42]. Semelsberger TA, Borup RL, Grene HL. Dimethyl ether (DME) as an alternative fuel. Journal of Power Sources 2006; 156: 497–511.

[43]. Li G. Dimethyl ether (DME): a new alternative fuel for diesel vehicle. Advanced Materials Research 2011; 156–157: 1014–1018.

[44]. Sezer I. Thermodynamic, performance and emission investigation of a diesel engine running on dimethyl ether and diethyl ether. International Journal of Thermal Sciences 2011; 50: 1594–1603.

[45]. Wang Y, Zhao Y, Yang Z. Dimethyl ether energy ratio effects in a dimethyl ether–diesel dual fuel premixed charge compression ignition engine. Applied Thermal Engineering 2013; 54: 481–487.

[46]. Ying W, Li H, Longbao Z, Wei L. Effects of DME pilot quantity on the performance of a DME PCCI–DI engine.

Energy Conversion and Management 2010; 51: 648–654.

[47]. Chen Z, Konno M, Kajitani S. Performance and emissions of DI compression ignition engines fueled with dimethyl ether. JSME International Journal 2000; 43(1): 82–88.

[48]. Arcoumanis C, Bae C, Crookes R, Kinoshita E. The potential of di–methyl ether (DME) as an alternative fuel for compression–ignition engines: A review. Fuel 2008; 87(7): 1014–1030.

[49]. Taghavifar H, Khalilarya S, Mirhasani S, Jafarmadar S. Numerical energetic and exergetic analysis of CI diesel engine performance for different fuels of hydrogen, dimethyl ether, and diesel under various engine speeds. International Journal of Hydrogen Energy 2014; 39: 9515–9526.

[50]. Patil KR, Thipse SS. A comparative study of performance and exhaust emissions of CI engine fuelled by neat DME and DME/DEE–diesel blends. Proceedings of International Conference on Advances in Mechanical Engineering 2013; 1–8.

[51]. Vispute KM, Pawar TJ. Study and prospects of di–methyl ether as an alternative fuel in C.I. engine: review. International Journal of Trend in Research and Development 2016; 3(4): 134–138.

[52]. Theinnoi K, Suksompong P, Temwutthikun W. Engine performance of dual fuel operation with in–cylinder injected diesel fuels and in–port injected DME. Energy Procedia 2017; 142: 461–467.

[53]. Deepak KM, Karthick M, Dineshbabu D, Srikanth P, Ramachandran MG. Investigation on the effect of dimethyl ether in compression ignition engine. International Journal of Innovative Research in Science, Engineering and Technology 2015; 4(2): 401–407.

[54]. Kajitani S. A study of low compression ratio diesel engines operated with neat dimethyl ether (DME). JSME TED Newsletter 2004; 42: 1–14.

[55]. Hewu W, Longbao Z. Performance of a direct injection diesel engine fuelled with a dimethyl ether/diesel blend. Journal of Automobile Engineering 2003; 217(9): 819–824.

[56]. Prabhakaran B, Thennarasu P, Karthick S. Performance and characteristics of a CI engine using DME (Dimethyl Ether). International Journal of Innovative Research in Science, Engineering and Technology 2015; 4(2): 31–34.

[57]. Kajitani S, Chen Z. Fundamental research on next generation fuel (dimethyl ether) engines. Journal of Scientific & Industrial Research 2003; 62: 133–144.

[58]. Abhishek, Rahul K, Santosh K, Martha O. Blending impacts of biogas and dimethyl ether (DME) on compressed ignition engine. International Research Journal of Engineering and Technology 2017; 4(4): 2174–2177.

[59]. Loganathan M, Anbarasu A, Velmurugan A. Emission characteristics of jatropha–ethanol and jatropha–dimethyl ether fuel blends on a DI diesel engine. Journal of Mechanical Engineering 2012; 42(1): 38–46.

[60]. Kim HJ, Park SH. Optimization study on exhaust emissions and fuel consumption in a dimethyl ether (DME) fueled diesel engine. Fuel 2016; 182: 541–549.

[61]. Park SH, Shin D, Park J. Effect of ethanol fraction on the combustion and emission characteristics of a dimethyl ether–ethanol dual–fuel reactivity controlled compression ignition engine. Applied Energy 2016; 182: 243–252.

[62]. Geng P, Cao E, Tan Q, Wie L. Effects of alternative fuels on the combustion characteristics and emission products from diesel engines: A review. Renewable and Sustainable Energy Reviews 2017; 71: 523–534.

[63]. Loganathan M, Anbarasu A, Velmurugan A. Emission characteristics of jatropha–dimethyl ether fuel blends on a DI diesel engine. International Journal of Scientific & Technology Research 2012; 1(8): 28–32.

[64]. Zhao Y, Wang Y, Li D, Lei X, Liu S. Combustion and emission characteristics of a DME (dimethyl ether)–diesel dual fuel premixed charge compression ignition engine with EGR (exhaust gas recirculation). Energy 2014; 72: 608–617.

[65]. Hou J, Wen Z, Jiang Z, Qiao X. Study on combustion and emissions of a turbocharged compression ignition engine fueled with dimethyl ether and biodiesel blends. Journal of the Energy Institute 2014; 87: 102–113.

[66]. Ying W, Longbao Z, Hewu W. Diesel emission improvements by the use of oxygenated DME/diesel blend fuels. Atmospheric Environment 2006; 40: 2313–2320.

[67]. Xinling L, Zhen H. Emission reduction potential of using gas–to–liquid and dimethyl ether fuels on a turbocharged diesel engine. Science of the Total Environment 2009; 407: 2234–2244.

[68]. Kim HJ, Park SH. Optimization study on exhaust emissions and fuel consumption in a dimethyl ether (DME) fueled diesel engine. Fuel 2016; 182: 541–549.

[69]. Park SH, Shin D, Park J. Effect of ethanol fraction on the combustion and emission characteristics of a dimethyl ether–ethanol dual–fuel reactivity controlled compression ignition engine. Applied Energy 2016; 182: 243–252.

[70]. Yanju W, Kun W, Wenrui W, Shenghua L, Xiao C, Yajing Y, Shanwen B. Comparison study on the emission characteristics of diesel– and dimethyl ether–originated particulate matters. Applied Energy 2014; 130, 357–369.

[71]. Wang Y, Zhao Y, Xiao F, Li D. Combustion and emission characteristics of a diesel engine with DME as port premixing fuel under different injection timing. Energy Conversion and Management 2014; 77: 52–60.

[72]. Park SH, Kim HJ, Lee CS. Effects of dimethyl–ether (DME) spray behavior in the cylinder on the combustion and exhaust emissions characteristics of a high speed diesel engine. Fuel Processing Technology 2010; 91: 504–513.

[73]. Thomas G, Feng B, Veeraragavan A, Cleary MJ, Drinnan N. Emissions from DME combustion in diesel engines and their implications on meeting future emission norms: A review. Fuel Processing Technology 2014; 119: 286–304.

[74]. Yoon SH, Han SC, Lee CS. Effects of high EGR rate on dimethyl ether (DME) combustion and pollutant emission characteristics in a direct injection diesel engine. Energies 2013; 6: 5157–5167.

[75]. Roh HG, Lee D, Lee CS. Impact of DME–biodiesel, diesel–biodiesel and diesel fuels on the combustion and emission reduction characteristics of a CI engine according to pilot and single injection strategies. Journal of the Energy Institute 2015; 88: 376–385.

[76]. Zhu Z, Li DK, Liu J, Wei YJ, Liu SH. Investigation on the regulated and unregulated emissions of a DME engine under different injection timing. Applied Thermal Engineering 2012; 35: 9–14.

[77]. Park SH, Yoon SH, Cha J, Lee CS. Mixing effects of biogas and dimethyl ether (DME) on combustion and emission characteristics of DME fueled high–speed diesel engine. Energy 2014; 66: 413–422.

[78]. Bogdan J, Nicolae B, Călin I, Vlad BN. Study of emissions for a compression ignition engine fueled with a mix of DME and diesel. Materials Science and Engineering 2017; 252: 1–9.

[79]. Kim HJ, Park SW, Lee CS. Numerical and experimental study on the combustion and emission characteristics of a dimethyl ether (DME) fueled compression ignition engine. Oil & Gas Science and Technology 2012; 67(3): 479–489.

[80]. Wang HW, Zhou LB, Jiang DM, Huang ZH. Study on the performance and emissions of a compression ignition engine fuelled with dimethyl ether. Journal of Automotive Engineering 2000; 214: 101–106.

[81]. Wang Y, Liu H, Huang Z, Liu Z. Study on combustion and emission of a dimethyl ether–diesel dual fuel premixed charge compression ignition combustion engine with LPG (liquefied petroleum gas) as ignition inhibitor. Energy 2016; 96: 278–285.

[82]. Kakoeea A, Gharehghani A. Comparative study of hydrogen addition effects on the natural–gas/diesel and natural–gas/dimethyl–ether reactivity controlled compression ignition mode of operation. Energy Conversion and Management 2019; 196: 92–104.